JOC The Journal of Organic Chemistry

Article

pubs.acs.org/joc

Synthetic and Quantum Mechanical Studies into the *N*-Heterocyclic Carbene Catalyzed (4 + 2) Cycloaddition

Sarah J. Ryan,[†] Andreas Stasch,[†] Michael N. Paddon-Row,*[,‡] and David W. Lupton*[,†]

[†]School of Chemistry, Monash University, Clayton 3800, Victoria, Australia

[‡]School of Chemistry, University of New South Wales, Sydney 2052, New South Wales, Australia

Supporting Information

ABSTRACT: The *N*-heterocyclic carbene catalyzed (4 + 2) cycloaddition between α,β-unsaturated acid fluorides and TMS dienol ethers provides cyclohexene fused β-lactone intermediates stable below −20 °C. These can be intercepted reductively or with organolithium reagents to produce diastereomerically pure cyclohexenes (>20:1 dr) with up to four contiguous stereocenters. The mechanism has been investigated using theoretical calculations and by examining secondary kinetic isotope effects. Together these studies implicate the formation of a diastereomerically pure β-lactone intermediate by a stepwise (4 + 2) cycloaddition involving Michael addition, aldol cyclization, and lactonization.

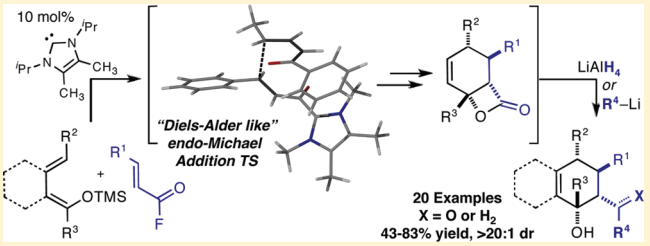

INTRODUCTION

N-Heterocyclic carbenes (NHCs) have enabled a wealth of discoveries in transition metal and organocatalysis.[1] As organocatalysts they provide access to an array of reactive intermediates,[2−6] while being compatible with co-catalysts and stoichiometric reagents.[7] As a consequence of such diverse reactivity, the design of transformations that target a specific mode of NHC-catalysis can be difficult. To address this challenge, increased understanding of the fundamental parameters that underpin the viability of NHC-catalysis is required.[8,9]

Recently, we reported the first all-carbon NHC-catalyzed (4 + 2) cycloaddition between TMS dienol ethers **1** and acid fluorides **2**.[5d] Central to the success of this transformation was the use of high nucleophilicity NHCs,[8a] which substitute at ester oxidation state starting materials, such as **2**. The reaction bears many of the hallmarks of more well-known (4 + 2) cycloadditions,[10,11] generating functionalized cyclohexadienes (i.e., **3**) in a stereochemically predictable fashion (eq 1). While this reaction has many positive characteristics, its potential was only partially realized. Of particular interest was the prospect of (4 + 2) cycloadditions that avoid decarboxylation of the putative β-lactone intermediate **4**. β-Lactones have interesting reactivity and are implicated in a range of NHC-mediated processes, with both isolation and decarboxylation reported.[12] We postulated that, through judicious control of the reaction conditions, it should be possible to achieve ring opening and hence deliver densely functionalized cyclohexenes (i.e., **5**) (eq 2). Beyond novelty, such reactions would provide access to complex materials suited to the assembly of natural and designed targets.

To realize these goals we commenced by re-examining the NHC-catalyzed (4 + 2) cycloaddition/decarboxylation (eq 1), using quantum mechanical and kinetic approaches. It was hoped that an improved mechanistic picture would inform the

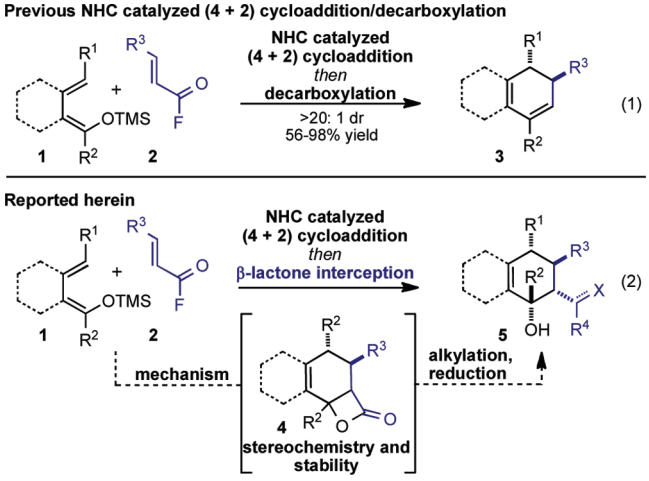

rational design of non-decarboxylative processes. Further motivating this study was the limited attention acyl azolium catalysis has received computationally.[9d−f] Herein we report quantum mechanical studies into the NHC-catalyzed (4 + 2) cycloaddition. Through these studies it has been possible to develop two new transformations that avoid decarboxylation of β-lactone **4** (eq 2).

Background. The NHC-catalyzed (4 + 2) cycloaddition/decarboxylation reaction can be rationalized by a number of mechanisms. In all, the first step presumably involves formation of dieneolate **6** and α,β-unsaturated acyl azolium **7** by NHC-mediated defluorination/desilylation (Scheme 1).[13] C−C bond formation can then occur in a stepwise or concerted

Received: December 7, 2011
Published: December 12, 2011

   dx.doi.org/10.1021/jo202500k | J. Org. Chem. 2012, 77, 1113−1124

Scheme 1. Potential Reaction Pathways

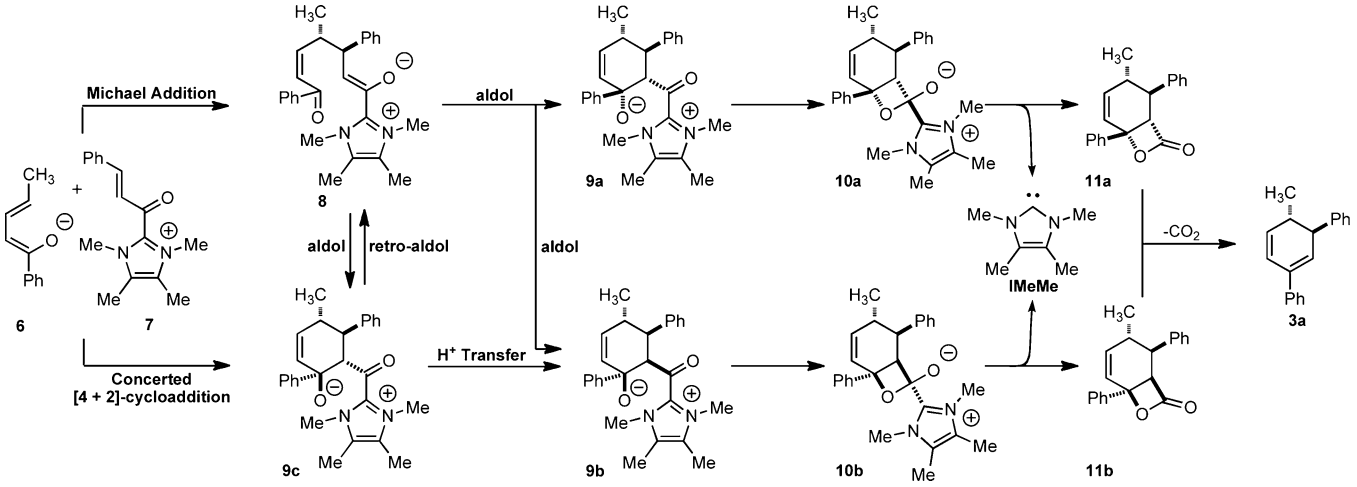

manner, to avail cyclohexenes **9a**, **b**, or **c**. From the stereochemical outcome of the reaction, *endo*-orientation between diene **6** and α,β-unsaturated acyl azolium **7** must occur in either path. For the concerted process this implicates formation of **9c**, with a *trans* arrangement between the alkoxide and acyl azolium, precluding direct access to the *cis* β-lactone. For this to occur **9c** must isomerize, via either a retro-aldol/aldol sequence[12e] or proton transfer, to provide cyclohexene **9a** or **b**, now capable of *cis* β-lactone formation. In contrast, if the reaction proceeds via conjugate adduct **8**, then rotational events followed by aldol cyclization provide direct access to either cyclohexene **9a** or **b**.

The catalytic cycle is completed by addition of the alkoxide into the acyl azolium to afford the tetrahedral intermediates **10a** or **b** and subsequent elimination of the NHC to provide lactones **11a** or **b**. Decarboxylation gives the cyclohexadiene **3a** and planarizes two stereogenic centers.

Computational experiments were undertaken using the structures shown in Scheme 1, which represent a good approximation for the actual experiments conducted. Central to these studies were (1) establishing the stepwise or concerted nature of the (4 + 2) cycloaddition, (2) predicting the stereochemistry of lactone **11** (**a**, **b**, or a mixture), and (3) identifying the stability of lactone **11**[14] and hence its potential to be exploited in reaction discovery.

All calculations were carried out using the Gaussian 09 software.[15] Unless stated otherwise, optimized geometries were calculated using the B3LYP hybrid functional[16,17] at the B3LYP/6-31+G(d) level of theory, using water as solvent with the polarizable continuum method (PCM).[18] Free energies and enthalpies in the text refer to single-point energies calculated using the hybrid meta-GGA M06-2X[19] functional at the M06-2X/6-311+G(2df,p)//B3LYP/6-31+G(d) level of theory, hereafter abbreviated as M06-2X//B3LYP. Full details of the computational method are provided in the Supporting Information.

RESULTS AND DISCUSSION

Reactant Energies. The dienolate **6** can exist in either the s-*cis* or s-*trans* conformer. The s-cisoid dienolate anion, **s-*cis*-6**, has a near planar geometry, with the two C=C double bonds making a dihedral angle of 1°, while the phenyl ring is twisted 25° with respect to the diene unit (Figure 1A). Although the cisoid conformer is slightly less stable than the s-transoid conformer, **s-*trans*-6**, by 5.5 (free energy) and 5.7 (enthalpy) kJ mol^{-1}, only reactions of the former are considered, since the

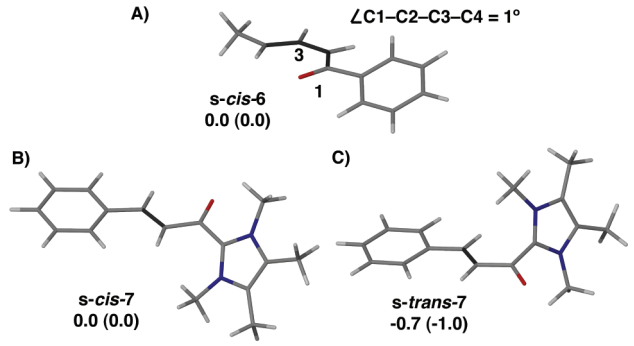

Figure 1. (A) **s-*cis*-6**. (B) **s-*cis*-7**. (C) **s-*trans*-7**. Free energies and enthalpies in kJ mol^{-1}. Enthalpies in parentheses.

experimental dienolates are constrained to the s-*cis* geometry as a consequence of annulation.

The α,β-unsaturated acyl azolium **7** also has two principal conformational isomers, namely, **s-*cis*-7** and **s-*trans*-7**, in which the carbonyl group is s-*cis* and s-*trans* to the alkene. The NHC moiety is significantly twisted from the C=O plane by approximately 41° in **s-*cis*-7** (Figure 1B) and 58° in **s-*trans*-7** (Figure 1C). The C=C−C=O group displays out-of-plane deviations of 7° and 12° in the s-*cis* and s-*trans* conformers, respectively. The **s-*trans*-7** conformer is slightly more stable than the **s-*cis*-7** conformer, by 0.7 (free energy) and 1.0 (enthalpy) kJ mole^{-1}.

Michael Addition. Despite many attempts, using various stratagems, a transition structure (TS) for a concerted Diels–Alder reaction between **6** and **7** could not be located. Instead, two TSs leading to Michael adducts were initially identified. The first, ***endo*-TS^1-8**, corresponds to *endo* addition of dienolate **s-*cis*-6** into dienophile **s-*cis*-7** (Figure 2A), while the second, ***exo*-TS^1-8**, corresponds to the *exo* addition (Figure 2B). Both TSs possess well-advanced C4···C5 bond formation, with lengths of 2.29 Å for the *endo* TS and 2.33 Å for the *exo* TS. In contrast, the C1···C6 distances of 3.40 Å (*endo*) and 3.80 Å (*exo*) show insignificant bond development between these centers. The small C1−C4−C5−C6 dihedral angles of −21° (***endo*-TS^1-8**) and 10° (***exo*-TS^1-8**), between the terminal carbon of the diene and the vinyl carbon of the dienophile, resemble a Diels–Alder TS. However, intrinsic reaction coordinate (IRC) analysis, carried out on both TSs, showed that they led to the Michael adducts ***endo*-8** (Figure 2C) and

dx.doi.org/10.1021/jo202500k | J. Org. Chem. 2012, 77, 1113–1124

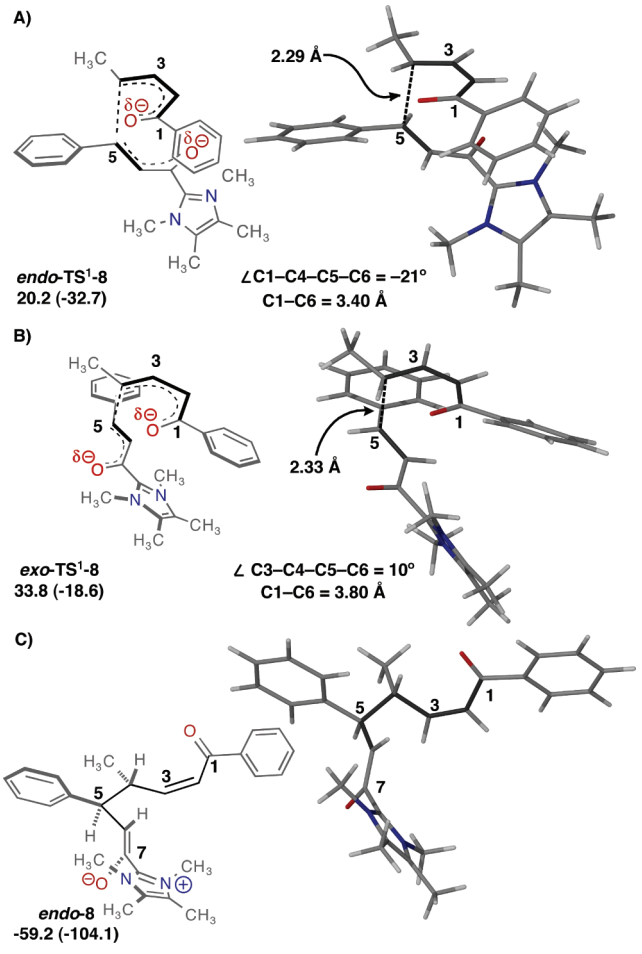

Figure 2. (A) *endo*-TS^1-8. (B) *exo*-TS^1-8. (C) *endo*-8. Free energies and enthalpies in kJ mol^{-1}. Enthalpies in parentheses.

exo-8. Mulliken population analyses of *endo*-TS^1-8 and *exo*-TS^1-8 revealed that −0.61*e* and −0.58*e*, respectively have been transferred from the erstwhile dienolate anion **6** to the dienophile **7**. This magnitude of charge transfer is consistent with a Michael reaction.[20]

In addition to *endo*-TS^1-8 and *exo*-TS^1-8, two higher energy TSs for both the *endo* and *exo* addition modes were located. These are conformational isomers with respect to rotation about the forming C4···C5 bond (see Supporting Information). All transition structures en route to **8** have the carbonyl group of acyl azolium **7** adopting an s-cisoid conformation with respect to the adjacent C═C double bond, i.e., **s-*cis*-7**. The conformational isomers of *endo*-TS^1-8 and *exo*-TS^1-8, in which the carbonyl group is s-transoid, are less stable by 17.1 and 8.1 kJ mol^{-1}, respectively, a consequence of increased steric interaction between the acyl azolium group and the dienolate.

Of the six Michael TSs *endo*-TS^1-8 is the most stable, with *exo*-TS^1-8 lying 13.6 kJ mol^{-1} higher in free energy and 14.1 kJ mol^{-1} higher in enthalpy. Thus, predominant formation (99%) of *endo*-8 is predicted. This high *endo* selectivity is based on the assumption that the Michael addition is irreversible as was observed in the previously reported transformation and mirrored in the cycloadditions described[5d] herein (*vide infra*).

The activation enthalpy for Michael addition via *endo*-TS^1-8 is −32.7 kJ mol^{-1} relative to the isolated reactants, the negative sign signifying the existence of a pre-TS complex, **pre-*endo*-TS^1-8**, which was duly located. The free energy of activation and enthalpy, relative to this complex, are 16.4 and 5.5 kJ mol^{-1}, respectively.

Aldol Cyclization and Lactonization. Having established Michael addition to afford *endo*-8, it remained to identify the events that allow cyclization, lactonization, and decarboxylation. Direct aldol cyclization of *endo*-8 via **TS-9c** to give cyclohexene **9c** is endergonic, by 53.1 kJ mol^{-1}, with 69.9 kJ mol^{-1} free energy of activation.

Since **9c** is incapable of availing a *cis* β-lactone and its formation is highly reversible, rotational isomers of *endo*-8 were examined to provide access to *cis* fused β-lactones **11a** and **b**. Three plausible pathways were identified (Figure 3). The first arises from ca. 180° rotation about the C3−C4 bond to afford **8a′** in which the C4-methyl now occupies the interior bounded by the butene group (Figure 3A). The second arises from rotation about the C1−C2 bond of around 180° to afford **8a**, in which the benzoyl carbonyl group is in an s-*trans* arrangement with the butene double bond (Figure 3B), while the final pathway is dominated by a 180° rotation about the C5−C6 bond to afford **8b** (Figure 3C). The structure of **8b** is similar to that which would be formed by Michael addition of the Z-dienophile. Ultimately, the first two intermediates **8a′** and **8a** lead to **10a**, in which the C5-phenyl and acyl azolium are *trans*, while **8b** delivers the *cis* product **10b**. The rotation of *endo*-8 to give **8a′**, **8a**, and **8b** occurs via **TS-8a′**, **TS-8a**, and **TS-8b** with activation free energies (enthalpies) of 36.0 (20.4), 10.5 (2.1), and 24.6 (18.0) kJ mol^{-1}, respectively.

The Michael adducts **8a′**, **8a**, and **8b** cyclize via transition structures **TS-9a**, **TS^{8a}-10a**, and **TS-10b** (Figure 3D−F), respectively. All three TSs display well-advanced C1···C6 bond formation, ranging from 1.964 Å, for **TS-9a** (Figure 3D), to 1.866 Å for **TS^{8a}-10a** (Figure 3E). IRC analyses showed that **TS-9a** leads to aldol product **9a**, with a C1−C6 bond length of 1.644 Å and a 2.652 Å distance between (C1)O and C7. In contrast, IRC analyses on the product-forming coordinates from **TS^{8a}-10a** and **TS-10b** revealed that they lead to the lactol tetrahedral intermediates **10a** and **10b**, without passing through the aldol products **9a** and **9b**. Bond formation between (C1)O and C7 had clearly occurred with lengths of 1.553 Å for **10a** and 1.548 Å for **10b**.

Conversion of the aldol product **9a** to lactol tetrahedral intermediate **10a** (Figure 4B) proceeds via **TS^{9a}-10a** (Figure 4A). This TS lies only 5.5 kJ mol^{-1} above **9a** in free energy and its geometry, particularly at the reaction center involving (C1)O−C7 bond formation, is remarkably similar to that of **9a**. The (C1)O···C7 distance of 2.504 Å in **TS^{9a}-10a** is only 0.15 Å smaller than the value of 2.652 Å in **9a** and the C1···C6 distance has shortened, from 1.644 Å in **9a**, to 1.606 Å. The (C1)O−C1−C6−C7 dihedral angle of 31° in **TS^{9a}-10a** is 6° smaller than that of **9a**, suggesting that torsional motion about the C1−C6 bond in the TS may play an important role in bond formation, since this dihedral angle in lactol tetrahedral intermediate **10a** is only 4°. Indeed, the imaginary frequency associated with the transition vector in **TS^{9a}-10a** is only 24 *i* cm^{-1}. An order of magnitude lower than that normally associated with bond formation but typical for rotational barriers. Thus, the transition vector is very delocalized, involving motions of many atoms, but one may clearly identify torsional motion about the C1−C6 bond, together with a small contribution from (C1)O···C7 stretching vibration. Unfortunately, IRC calculations on **TS^{9a}-10a** failed. However, relaxed potential energy scans, using (C1)O···C7 as the variable, demonstrated that the

dx.doi.org/10.1021/jo202500k | J. Org. Chem. 2012, 77, 1113−1124

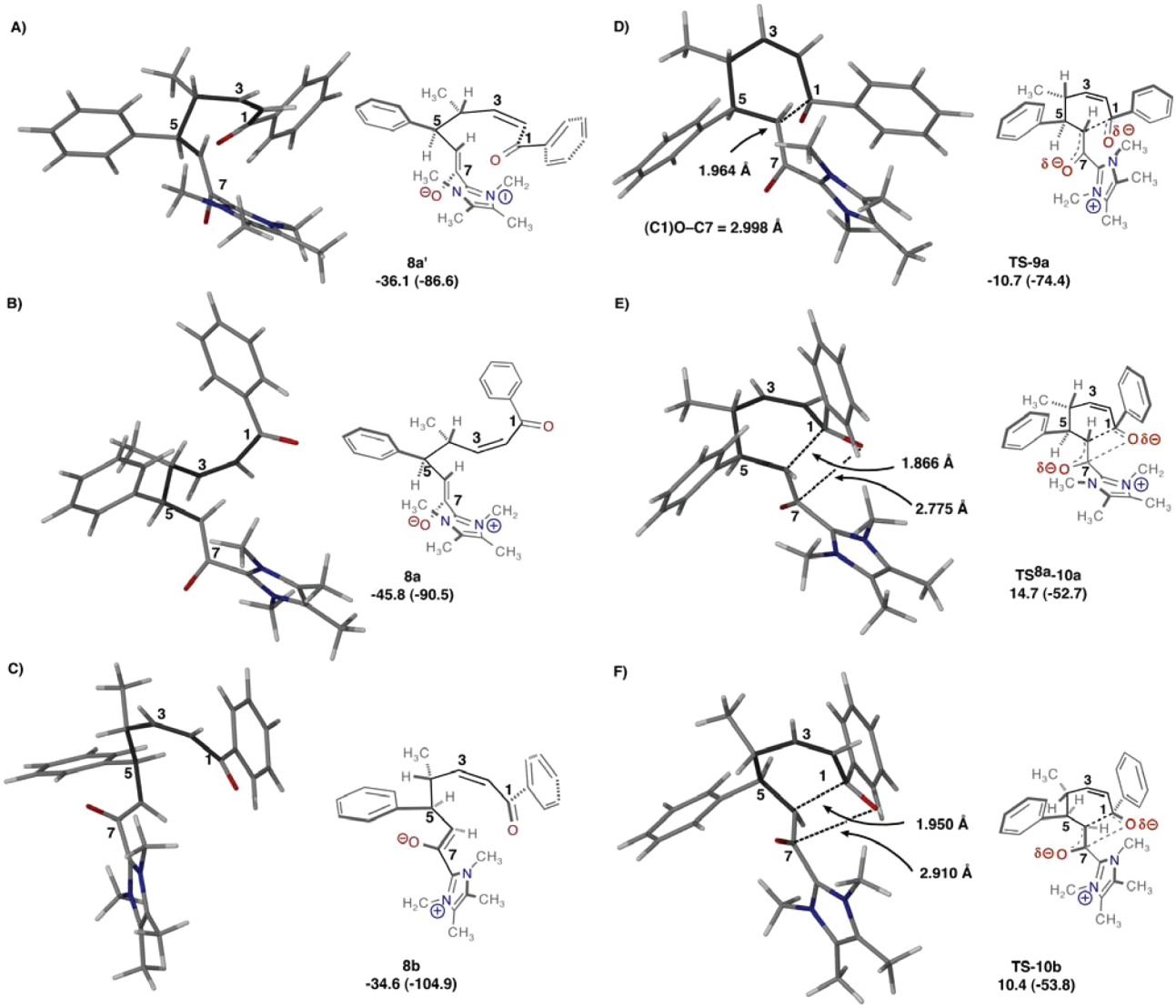

Figure 3. Rotational isomers of ***endo*-8** to afford (A) **8a′**, (B) **8a**, and (C) **8b** and transition structures for their cyclization (D) **TS-9a**, (E) **TS^{8a}-10a**, and (F) **TS-10b**. Free energies and enthalpies in kJ mol^{-1}. Enthalpies in parentheses.

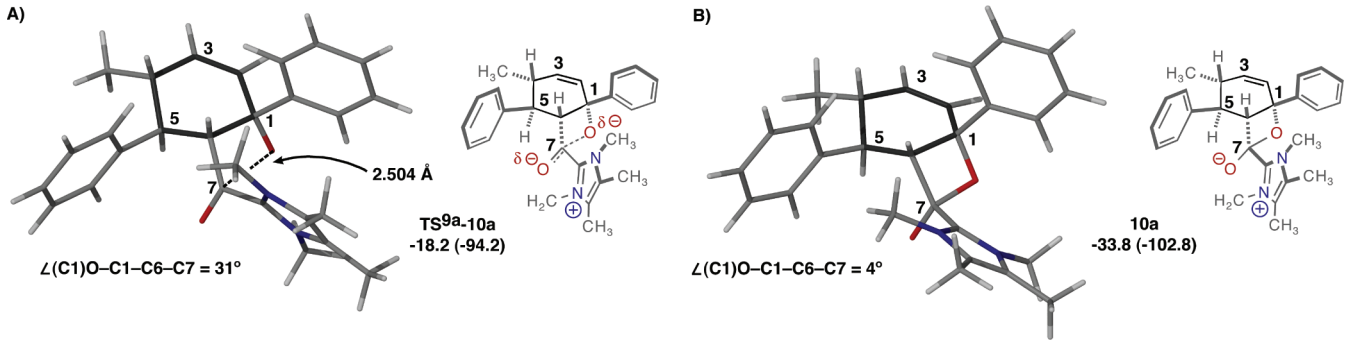

Figure 4. (A) **TS^{9a}-10a**. (B) **10a**. Free energies and enthalpies in kJ mol^{-1}. Enthalpies in are parentheses.

potential energy decreased, monotonically, from **TS^{9a}-10a** to **10a**, the same intermediate produced from **TS^{8a}-10a**. Thus, the two Michael adducts **8a′** and **8a** ultimately lead to the same tetrahedral intermediate **10a**.

Elimination of the NHC from the lactol tetrahedral intermediates **10a** and **10b** proceeds via **TS-11a** and **TS-11b**, with activation free energies (enthalpies) of 58.0 (60.2) and 51.2 (55.8), respectively, to provide lactones **11a** and **11b**. Lactone formation is exergonic with reaction free energies of −9.8 kJ mol^{-1} for **11a** and −24.5 kJ mol^{-1} for **11b**. This final step in the NHC-catalyzed (4 + 2) cycloaddition proceeds over the highest energy barrier and will therefore determine the ratio of lactones produced. Thus, Curtin−Hammett analysis of this step provides a $\Delta\Delta G^{\ddagger}$ between **TS-11a** and **TS-11b** of

dx.doi.org/10.1021/jo202500k | J. Org. Chem. 2012, 77, 1113−1124

4.2 kJ mol^{-1}, which if the reaction proceeds at −50 °C (*vide infra*) indicates that lactone **11a** should be the major product, with a **11a**:**11b** ratio of 9.6:1.

Decarboxylation. **TS^{11a}-3a** and **TS^{11b}-3a**, TSs for the decarboxylation of lactones **11a** and **11b**, are interesting in that although IRC analyses confirmed their concertedness, they are extremely asynchronous (Figure 5). This observation is

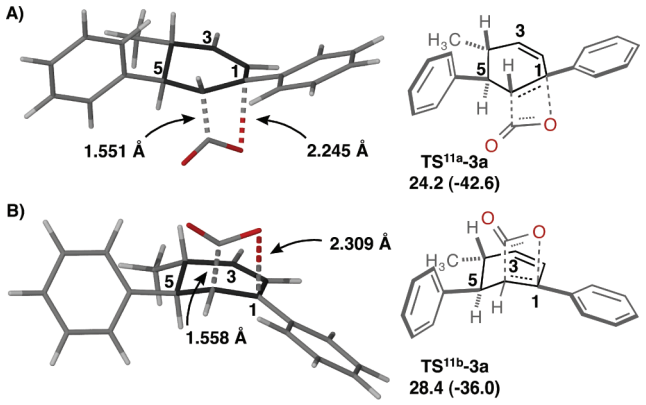

Figure 5. Decarboxylation of lactones **11a** and **11b** via (A) **TS^{11a}-3a** and (B) **TS^{11b}-3a**. Free energies and enthalpies in kJ mol^{-1}. Enthalpies in parentheses.

supported by previous computational[14] and kinetic studies.[21] Whereas the C1−O bond has substantially lengthened by about 0.7 Å in the TSs compared to that in the lactone reactants, the C6−C7 bond length in the TSs has increased by only about 0.03 Å. This high degree of asynchronicity is reflected in the transition vector, which is dominated by the C1−O stretching vibrations. This near unilateral scission of the C−O bond in the TS results in significant migration of negative charge to the embryonic CO_2 moiety, amounting to −0.46*e* and −0.38*e* in **TS^{11a}-3a** and **TS^{11b}-3a**, respectively. As a consequence, the dipole moments of the TSs are substantially larger than those of the lactone reactants, 13.2 and 12.9 D in **TS^{11a}-3a** and **TS^{11b}-3a**, respectively, and 6.7 and 6.1 D in **11a** and **11b**. This increased polarity in the TSs, compared to the reactant lactones, suggests that the decarboxylation rate should be strongly dependent on solvent polarity (*vide infra*). The decarboxylation reactions are fairly strongly exergonic and exothermic. The free energies (enthalpies) of reactions are −96.7 (−53.9) and −93.0 (−51.1) kJ mol^{-1} for **11a** and **11b**, respectively. The decarboxylation activation free energies for **11a** and **11b** are 90.8 and 88.0 kJ mol^{-1}, respectively. The effect of fusing a six-membered ring to lactone **11a** on the decarboxylation activation energy was investigated using **11c**, a system studied experimentally. The free energy of activation for the decarboxylation of this lactone is 91.5 kJ mol^{-1}, only 0.7 kJ mol^{-1} larger than that for **11a** (eq 3).

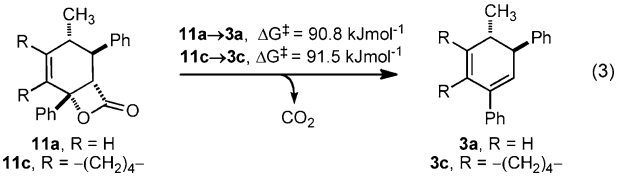

(3)

While these studies suggest that the *β*-lactone is sufficiently stable to be exploited in reaction discovery and that reasonable stereoselectivity for **11a** over **11b** should be observed, we decided to further examine the accuracy of the M06-2X//B3LYP model chemistry in predicting decarboxylation activation energies. When the more accurate multilevel *ab initio* G4[22] and G4(MP2)[23] methods were applied with the more tractable lactone **11d** (eq 4), the activation free energies were found to be 83.8 (Table 1, entry 1) and 84.9 kJ mol^{-1}

Table 1. Decarboxylation of Lactones 11d and e

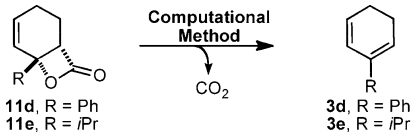

(4)

entry	computational method	solvent	11	$\Delta G^{\ddagger}$ (kJ mol^{-1})
1	G4	H_2O	**d**	83.8
2	G4(MP2)	H_2O	**d**	84.9
3	M06-2X//B3LYP	H_2O	**d**	88.7
4	G4(MP2)	toluene	**d**	110.3
5	M06-2X//B3LYP	toluene	**d**	114.2
6	G4	H_2O	**e**	80.0
7	G4(MP2)	H_2O	**e**	80.9
8	M06-2X//B3LYP	H_2O	**e**	88.5

(Table 1, entry 2), respectively. In comparison, M06-2X//B3LYP predicted 88.7 kJ mol^{-1} (Table 1, entry 3). Replacement of the phenyl substituent by the isopropyl (i.e., **11e** cf. **11d**) resulted in a small decrease in activation free energy to 80.0 using the G4 method (Table 1, entry 6), 80.9 using G4(MP2) (Table 1, entry 7), and 88.5 using M06-2X//B3LYP (Table 1, entry 8) kJ mol^{-1}.

These results suggest that the M06-2X//B3LYP model chemistry is quite reliable for predicting activation free energies for the decarboxylation of *β*-lactones, with only a slight overestimation of ca. 7 kJ mol^{-1}. Comparing the *ab initio* methods, the moderately less accurate but computationally much faster G4(MP2) method gives almost identical results to the more demanding G4 method.

As mentioned, the increased polarity of the decarboxylation TS compared to the reactant lactone suggests that the activation energy should increase with decreasing solvent polarity. Indeed, the free energy of activation for the decarboxylation of **11d** increases upon changing the PCM solvent from water to toluene. Thus, the G4(MP2) method predicts a 25.4 kJ mol^{-1} increase in activation energy (Table 1, entry 2 cf. 4), an increase almost the same as that calculated using M06-2X//B3LYP (Table 1, entry 3 cf. 5). To examine this experimentally the reaction was trialed using a range of solvents less polar than THF. Unfortunately, in all cases competing *O*-acylation of the dienolate anion **6** by the *α*,*β*-unsaturated acyl azolium **7** precluded identification of this solvent effect.

Reaction Coordinate. The important reaction pathways in the NHC-catalyzed (4 + 2) cycloaddition are summarized in Figure 6. Initially, Michael-addition between acyl azolium **7** and diene **6** is predicted via ***endo*-TS^{1}-8**, a transition structure that resembles a Diels−Alder TS but that leads to Michael adduct ***endo*-8**. The next lowest TS has an *exo* orientation between acyl azolium **7** and diene **6** with a relative energy difference predicting 99% ***endo*-8**. This intermediate can directly cyclize via **TS-9c** to provide the Diels−Alder adduct **9c**. This occurs with a high-energy barrier, is endogonic, and provides an intermediate unable to form a *cis* *β*-lactone. In contrast, three

dx.doi.org/10.1021/jo202500k | J. Org. Chem. 2012, 77, 1113−1124

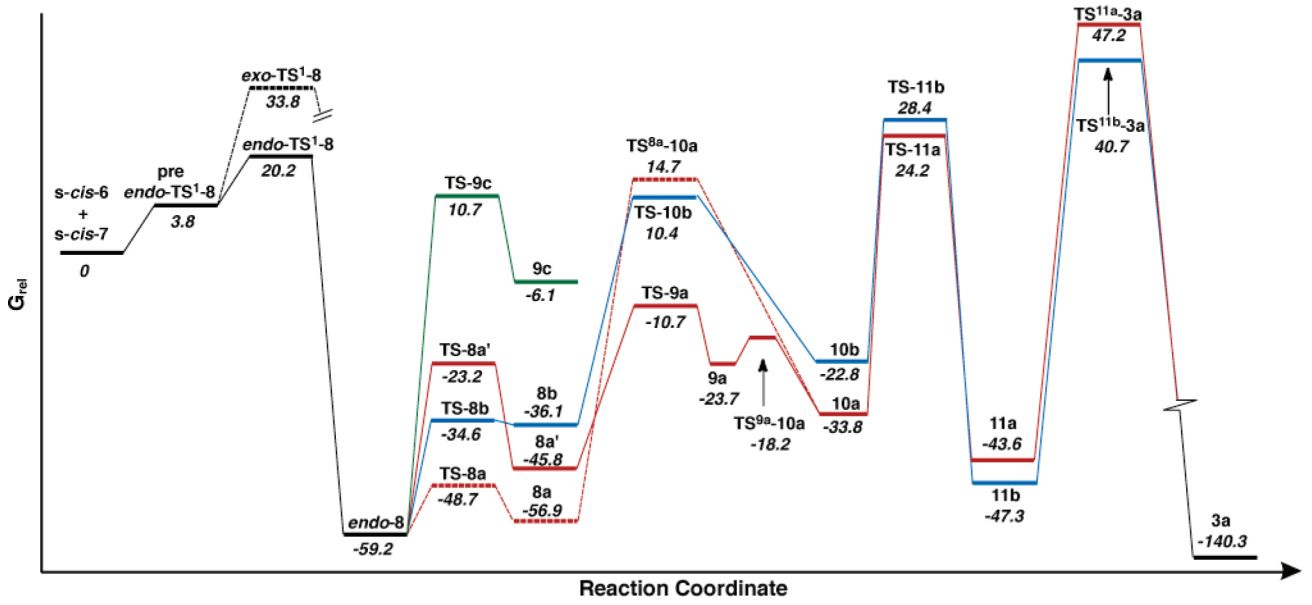

Figure 6. M06-2X//B3LYP free energies of stationary points along the reaction coordinate in kJ mol^{-1}.

rotational pathways from ***endo*-8** lead to intermediates **8a′**, **8a**, and **8b**, which are ultimately capable of providing *cis* β-lactones. Two pathways provide lactol intermediate **10a**, while a third avails **10b**. Although all three pathways are viable energetically, the lower barrier for loss of the NHC to provide lactone **11a** compared to **11b** ($\Delta\Delta G^{\ddagger}$ of 4.2 kJ mol^{-1}) suggests that **11a** will form with around 10:1 selectivity. Thus, studies of the (4 + 2) cycloaddition indicate a stepwise mechanism that should avail the β-lactone intermediate **11a** in which the lactone is *trans* to the C5-phenyl group. The prediction that the initial reaction step is a Michael addition rather than a concerted Diels–Alder addition can be tested experimentally, through measurement of H/D secondary kinetic isotope effects (SKIEs) at the α and β positions of the acyl azolium.[24] The B3LYP/6-31+G(d) calculated k_H/k_D SKIEs are 1.028 (α) and 0.934 (β) for Michael addition. For a concerted Diels–Alder inverse SKIEs would be expected at both sites (*vide infra*).

Finally, the free energy of activation for the decarboxylation of **11a** is predicted to be 90.8 kJ mol^{-1} in water. Higher level calculations on smaller model system (Table 1) suggest that M06-2X//B3LYP overestimates the barrier by about 7 kJ mol^{-1}. Thus the activation free energy for the decarboxylation of **11a** is likely to be around 84 kJ mol^{-1}. Using standard TS theory with a unity value for the transmission coefficient, this gives a predicted half-life for lactone **11a** of ca. 24 min at 0 °C. Thus, there exists a temperature window between β-lactone formation and decarboxylation, which can presumably be exploited synthetically.

Kinetic Isotope Studies. Synthetic studies commenced by examining the stepwise or concerted nature of the (4 + 2) cycloaddition using kinetic isotope effects. Although preliminary studies focused on primary $^{12}C/^{13}C$ KIEs, established using natural abundance techniques,[25] this approach gave unreliable results due to partial aromatization over the time frame required to acquire data. To address these limitations we chose to use secondary H/D KIEs determined using isotopically enriched starting materials. Thus, α,β-unsaturated acid fluorides **2b** (α-D) and **2c** (β-D) were prepared and the α- and β-SKIEs were determined using internal competition studies (eqs 5 and 6).[26] Using this approach the α-SKIE was found to

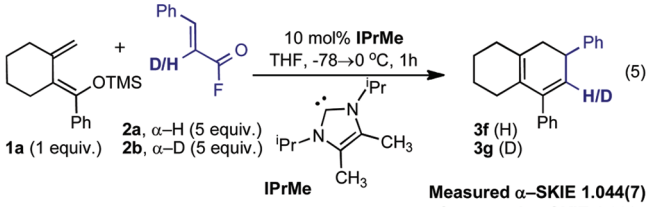

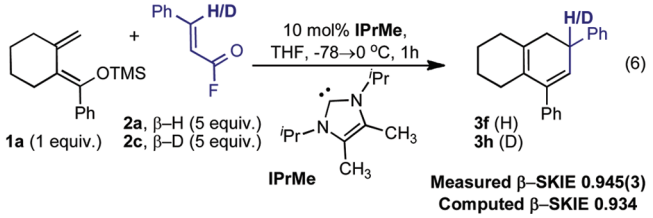

be 1.044(7), while the β-SKIE was 0.945(3). Qualitatively, these results support a stepwise mechanism in which rehybridization of the β-carbon from sp^2 to sp^3 occurs, while the α-position retains sp^2 character. If the reaction was concerted then inverse α- and β-SKIEs would be expected.[26,27] In addition, good agreement between the computational and experimentally determined SKIEs were observed, further supporting a stepwise mechanism.

Synthetic Studies. From the computational studies it was apparent that the β-lactone intermediate is relatively stable, with decarboxylation likely occurring as the reaction warms or during workup. In addition, high levels of selectivity for formation of the β-lactone intermediate **11a**, in which the lactone is *trans* to the C5-phenyl group, should be observed. If these predictions are correct, then interception, prior to decarboxylation, should provide access to densely functionalized cyclohexenes with up to 4-contiguous stereogenic centers, with good stereoselectivity.

***β*-Lactone Reduction.** To test these predictions we began by exploring the reduction of the β-lactone intermediate. Thus, dienol ether **1a**[28] and acid fluoride **2a** were exposed to 10 mol % **IPrMe** at −78 °C and the reaction warmed to 0 °C before being quenched with $LiAlH_4$. ^{1}H NMR analysis showed that a

dx.doi.org/10.1021/jo202500k | J. Org. Chem. 2012, 77, 1113–1124

Table 2. Investigation of Decarboxylation Temperature

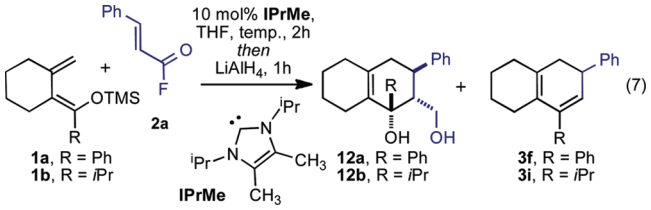

entry	temp (°C)	diene	12:3[a]	yield 12[b]
1	−78 → 0	**1a**	3:2	41
2	−78 → −10	**1a**	10:1	50
3	**−78 → −20**	**1a**	**100:0**	**71**
4	−78 → −50	**1a**	100:0	71
5	−78 → −10	**1b**	6:1	40
6	−78 → −20	**1b**	100:0	83

[a]Ratio determined by ^{1}H NMR analysis of unpurified material. [b]Isolated yield following chromatography.

3:2 ratio of diol **12a** and diene **3f** had formed (Table 2, entry 1). This ratio is in keeping with the computationally predicted half-life of the β-lactone at this temperature. Maintaining the temperature at −10 °C increased selectivity for the formation of **12a** (10:1) which was now isolated in 50% yield (Table 2, entry 2). To ensure that internal heating upon addition of the reducing agent was not driving decarboxylation, the experiment was repeated with the reaction recooled to −78 °C prior to reduction. An identical ratio of diol to diene was observed. Finally, by ensuring the reaction was maintained below −20 °C decarboxylation was eliminated, and **12a** could now be isolated in 71% yield (Table 2, entry 3). To examine the temperature at which β-lactone formation occurs, the reaction was repeated with the temperature maintained at −50 °C, providing the identical outcome to the reaction conducted at −20 °C and highlighting the facile nature of the NHC-catalyzed (4 + 2) cycloaddition (Table 2, entry 4). When the reaction was maintained at −78 °C, it failed to reach completion after 2 h. Next we examined dienol ether **1b**, in which the phenyl (in **1a**) is replaced by an isopropyl group, to test the computationally predicted lowering of the decarboxylation activation energy (Table 1, entry 1 cf. 6). We found that decarboxylation of this material was slightly more significant at −10 °C than with dienol ether **1a** (Table 2, entry 2 cf. 5), although it was eliminated at −20 °C (Table 1, entry 6). While the origin of this effect is not obvious, it presumably indicates that the resonance stabilization of the aromatic group and the vinyl group are not additive, while the hyperconjugative and resonant effects are.

With a reliable method to access diol **12a** its relative stereochemistry could be determined. Initial NOE analysis indicated *trans* arrangement between the C5-phenyl group and the reduced β-lactone, as predicted computationally. The stereochemistry was unambiguously confirmed by single crystal X-ray structural analysis (Figure 7).

The scope of the reductive NHC-catalyzed (4 + 2) cycloaddition was examined with a range of TMS dienol ethers **1** and acid fluorides **2** (Table 3). Provided the reduction was performed below −20 °C the expected diols could be prepared without any decarboxylation. In addition, none of the diols derived from the lactone intermediates in which the phenyl group is *cis* to the lactone were observed, suggesting that the $\Delta\Delta G^{\ddagger}$ between **TS-11b** and **TS-11a** was somewhat

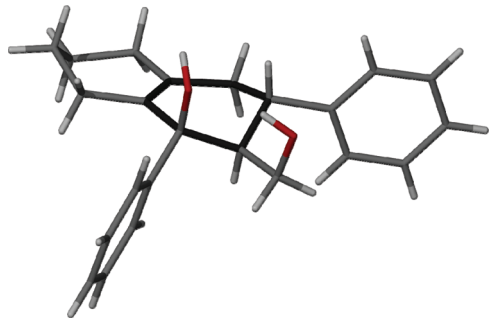

Figure 7. Molecular structure of **12a**.

Table 3. NHC-Catalyzed (4 + 2) Cycloaddition/Reduction[a]

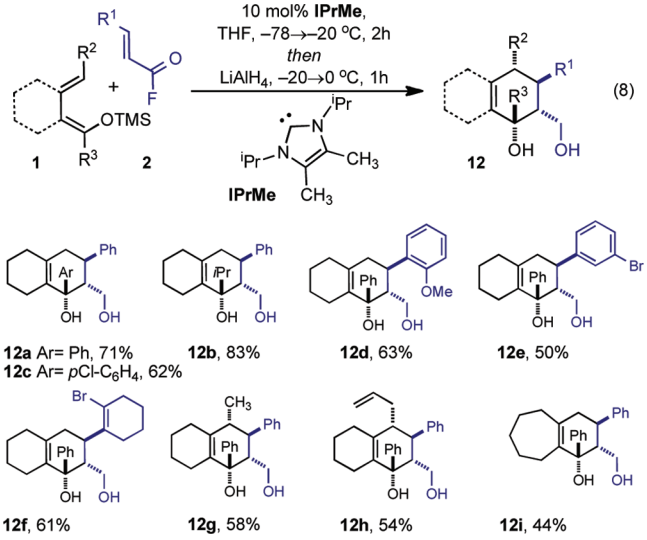

[a]All materials isolated as a single diastereoisomer as determined by ^{1}H NMR (>20:1 dr). Isolated yield following chromatography.

underestimated. When the R^2 substituent in the diene portion was not H (i.e., **1g** and **h**) cyclohexenes substituted at each carbon, with four new stereogenic centers, were generated in acceptable yields (i.e., **12f** and **g**) and as a single diastereoisomer.

β-Lactone Carbanion Addition. In addition to reduction of the β-lactone, nucleophilic ring opening was investigated. While heteroatom-based nucleophiles (O, N, or S) gave unsatisfactory results, carbon nucleophiles were far more useful. Using alkyl and aryl lithium reagents it was possible to introduce a large range of groups to the carbonyl of the β-lactone. In all cases only monosubstitution was observed (Table 4), implicating a stable β-lactol intermediate that upon workup provides the keto alcohol product **13**. The scope of this transformation was very broad with even sterically challenging nucleophiles such as the *t*Bu group able to add to the β-lactone in good yields (i.e., **13e**). Once more the reaction proceeds with exquisite stereoselectivity providing a single diastereomer, with up to four new stereogenic centers (i.e., **13k**).

CONCLUSIONS

Through computational and kinetic examination of the NHC-catalyzed (4 + 2) cycloaddition it has been possible to determine the key events associated with this reaction. The stereochemical outcome of the reaction is determined by Michael addition, via an *endo* TS, and aldol cyclization. The later predominantly provides the *trans* arrangement between

dx.doi.org/10.1021/jo202500k | J. Org. Chem. 2012, 77, 1113−1124

Table 4. NHC-Catalyzed (4 + 2) Cycloaddition/Carbanion Addition[a]

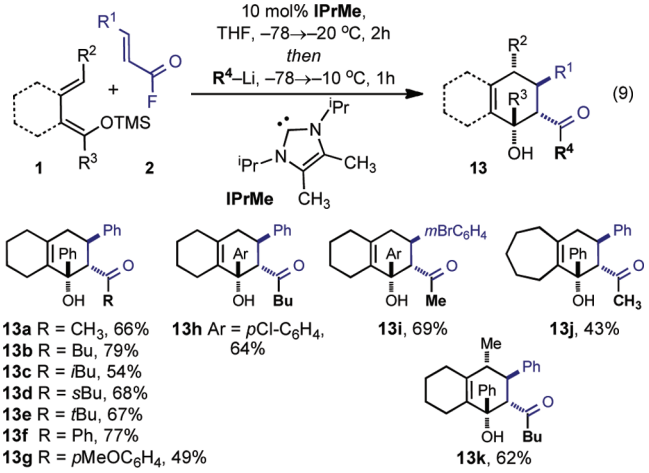

[a]All materials isolated as a single diastereoisomer as determined by ^{1}H NMR (>20:1 dr). Isolated yield following chromatography.

the lactone and C5-phenyl group, which is relayed into the β-lactone intermediate. Importantly, computational studies indicate that the β-lactone intermediate should be relatively stable, thereby allowing use in reaction discovery.

Synthetic studies support these computational predictions and have led to the identification of two new transformations. These transformations provide access to diastereomerically pure, functionalized cyclohexenes in good yields. In addition, these studies support the stereochemical models predicted computationally.

NHC catalysis is highly flexible, allowing diverse transformations to be developed. The ability to design and execute these reactions requires a thorough mechanistic understanding of the parameters pivotal to success. For NHC-catalysis to play a part in meeting the future challenges facing chemical synthesis, meaningful models of reactivity are required. Ongoing studies are focused on the discovery and rationalization of novel reactivity.

EXPERIMENTAL SECTION

General. Proton (^{1}H) and carbon (^{13}C) NMR spectra were recorded at 500 or 400 MHz for proton and 125 or 100 MHz for carbon nuclei. High resolution mass spectra (HRMS) (ESI) were recorded using NaI for accurate mass calibration. Flash column chromatography was performed on silica gel (LC60A, 40−63 μm silica media) using compressed air or nitrogen. Thin layer chromatography (TLC) was performed using plastic-backed plates coated with 0.2 mm silica. Eluted plates were visualized using a 254 nm UV lamp and/or by treatment with a suitable stain followed by heating. Tetrahydrofuran (THF) was distilled from sodium benzophenone ketyl, and dichloromethane was distilled from calcium hydride. Starting TMS dienol ethers were prepared according to the procedures of Lupton,[5d,28] acyl fluorides were prepared according to the procedure of Chen,[29] and IPrMe was prepared according to the procedure of Lyapkalo.[30] For computational procedures see Supporting Information.

Secondary Kinetic Isotope Effect Studies. Preparation of Deuterated Acid Fluorides. Following the procedure of Chen,[29] a mixture of α-D-(*E*)-cinnamic acid,[31] or β-D-(*E*)-cinnamic acid (10 mmol) and pyridine (2 mL) in CH_2Cl_2 (30 mL) was added to a stirred solution of 70% HF in pyridine (0.3 mL, 11 mmol) and DCC (2.06 g, 10 mmol) in CH_2Cl_2 (6 mL). The reaction mixture was stirred for 2 h at room temperature and filtered, and the volatiles were removed *in vacuo*. The crude residue was purified *via* distillation under reduced pressure to provide acid fluorides. α-D-(*E*)-Cinnamoyl fluoride (**2a**)[5d] has been reported previously.

***β*-D-(*E*)-Cinnamoyl fluoride (2c).** The acid precursor was prepared via hydrolysis of the corresponding ester, itself formed via a modified procedure of Gaffney[32] involving the Horner−Wadsworth−Emmons (HWE) reaction between triethylphosphonoacetate and benzaldehyde-α-D. IR ν_{max} 1796, 1616, 1449, 1206, 1107 ^{1}H NMR (500 MHz, $CDCl_3$) δ 7.57−7.55 (m, 2H), 7.48−7.42 (m, 3H), 6.35 (brd, J = 7.5 Hz, 1H); ^{13}C NMR (125 MHz, $CDCl_3$) δ 157.0 (d, J = 337 Hz), 132.9, 131.8, 129.1, 128.6, 128.5 (d, J = 80.3 Hz), 111.8 (d, J = 66.9 Hz); GC−MS (EI) m/z found $(M)^+$, 151.1, C_9H_6DFO requires $(M)^+$, 151.1

Secondary Kinetic Isotope Effects. TMS ether **1a** was reacted in the presence of a 1:1 mixture of cinnamoyl fluoride and either α-D-(*E*)-cinnamoyl fluoride **2b** (α SKIE) or β-D-(*E*)-cinnamoyl fluoride **2c**. Using approaches developed by Gajewski[26] secondary kinetic isotope effects (SKIEs) were determined by the comparison of enriched samples, taken to 10% conversion, with standard samples taken to complete conversion.[25,26] From these studies SKIEs for the α and β protons of the acid fluoride could be determined. To ensure consistency in the ratio of cinnamoyl fluoride **2a** to α- or β-D-(*E*)-cinnamoyl acid fluorides (**2b** or **c**) across both standard and enriched experiments, a solution containing 0.55 mmol of (*E*)-cinnamoyl fluoride **2a** and 0.55 mmol of α- or β-D-(*E*)-cinnamoyl fluoride in 11 mL of THF was prepared. From this mixture 1 mL (0.1 mmol, combined acyl fluoride) was transferred to a separate flask to conduct the standard experiment. The remaining 10 mL (1 mmol, combined acyl fluoride) was used in the enrichment experiment. The reaction mixtures were cooled to −78 °C, and TMS ether (0.1 mmol) was added followed by IPrMe (0.1 mL of a 0.1 M solution in THF). The mixtures were allowed to slowly warm to −10 °C over the period of 1 h. The volatiles were evaporated, and the crude residues were purified via flash column chromatography (1: 99, EtOAc/hexanes) to afford standard and enriched diene mixtures. For analysis see Supporting Information.

General Procedure for the NHC-Catalyzed (4 + 2) Cycloaddition/Reduction. A solution of IPrMe (0.1 M in THF, 0.2 mL, 0.02 mmol) was added to a stirred solution of TMS ether (0.2 mmol) and acid fluoride (0.2 mmol) in THF (3 mL) at −78 °C. The reaction mixture was allowed to warm to −20 °C over the period of 1 h and maintained between −20 and −30 °C for an additional 1 h. Lithium aluminum hydride (30 mg, 0.8 mmol) was then added. The reaction mixture was allowed to warm to room temperature after which time it was carefully quenched with water. The aqueous layer was extracted with ethyl acteate (3 × 10 mL), and the combined organic layers were dried ($MgSO_4$), filtered, and evaporated. The crude residue was purified *via* flash column chromatography (1:4 or 1:9 v/v EtOAc/hexanes) to afford the pure diols **12**.

(1*R*,2*R*,3*R*)-2-(Hydroxymethyl)-1,3-diphenyl-1,2,3,4,5,6,7,8-octahydronaphthalen-1-ol and (1*S*,2*S*,3*S*)-2-(Hydroxymethyl)-1,3-diphenyl-1,2,3,4,5,6,7,8-octahydronaphthalen-1-ol (12a). White solid, mp 144.7−148.5 °C; R_f 0.3 (1:4, v/v EtOAc/hexanes); IR ν_{max} 3307, 2928, 1446, 1046, 909; ^{1}H NMR (300 MHz, $CDCl_3$) δ 7.49−7.47 (m, 2H), 7.40−7.35 (m, 2H), 7.30 (d, J = 5.7 Hz, 4H), 7.28−7.19 (m, 2H), 3.51−3.39 (m, 3H), 3.19 (ddd, J = 10.5, 6.6, 3.6 Hz, 1H), 2.52−2.22 (m, 3H), 2.11−2.05 (m, 3H), 1.82−1.62 (m, 3H), 1.46−1.39 (m, 3H); ^{13}C NMR (75 MHz, $CDCl_3$) δ 146.1, 144.0, 133.2, 132.2, 128.6, 128.0, 127.9, 126.5, 126.4, 126.2, 80.1, 60.7, 52.0, 40.5, 38.5, 30.6, 25.0, 23.1, 22.7; HRMS (ESI) m/z found $(M + Na)^+$, 357.1824, $C_{23}H_{26}O_2$ requires $(M + Na)^+$, 357.1825

(1*R*,2*R*,3*R*)-2-(Hydroxymethyl)-1-isopropyl-3-phenyl-1,2,3,4,5,6,7,8-octahydronaphthalen-1-ol and (1*S*,2*S*,3*S*)-2-(Hydroxymethyl)-1-isopropyl-3-phenyl-1,2,3,4,5,6,7,8-octahydronaphthalen-1-ol (12b). White solid, mp 157.1−162.7 °C; R_f 0.3 (1:4, v/v EtOAc/hexanes); IR ν_{max} 3367, 2928, 1453, 1045, 1032, 909; ^{1}H NMR (400 MHz, $CDCl_3$) δ 7.26−7.19 (m, 4H), 7.16−7.12 (m, 1H), 3.87 (dd, J = 11.6, 1.6 Hz, 1H), 3.25 (dd, J = 11.6, 2.4 Hz, 1H), 2.95 (ddd, J = 16.4, 12.4, 4.4 Hz, 1H), 2.54 (br s, 1H), 2.19−2.03 (m, 3H), 1.93−1.84 (m, 5H), 1.74−1.65 (m, 2H), 1.50−1.44 (m, 3H), 0.98 (d, J = 7.2 Hz, 3H), 0.85 (d, J = 7.2 Hz, 3H); ^{13}C NMR (100 MHz,

dx.doi.org/10.1021/jo202500k | J. Org. Chem. 2012, 77, 1113−1124

$CDCl_3$) δ 145.3, 133.0, 132.1, 128.5, 127.8, 126.3, 78.8, 62.1, 46.3, 39.8, 39.0, 36.5, 31.1, 23.9, 23.4, 22.9, 18.1, 17.4; HRMS (ESI) m/z found $(M + Na)^+$, 323.1988, $C_{20}H_{28}O_2$ requires $(M + Na)^+$, 323.1982

(1*R*,2*R*,3*R*)-1-(4-Chlorophenyl)-2-(hydroxymethyl)-3-phenyl-1,2,3,4,5,6,7,8-octahydronaphthalen-1-ol and (1*S*,2*S*,3*S*)-1-(4-Chlorophenyl)-2-(hydroxymethyl)-3-phenyl-1,2,3,4,5,6,7,8-octahydronaphthalen-1-ol (12c). White solid, mp 199.5−200.2 °C (decomp.); R_f 0.3 (1:4, v/v EtOAc/hexanes); IR ν_{max} 3282, 2928, 1486, 1091, 1047, 908; ^{1}H NMR (500 MHz, $CDCl_3$) δ 7.41−7.40 (m, 2H), 7.33−7.28 (m, 5H), 7.24−7.21 (m, 2H), 3.73 (s, 1H), 3.41 (td, J = 12.0, 5.0 Hz, 1H), 3.37 (d, J = 12.0 Hz, 1H), 3.19−3.16 (m, 1H), 2.46−2.28 (m, 2H), 2.05−1.99 (m, 3H), 1.78−1.65 (m, 4H), 1.42−1.36 (m, 3H); ^{13}C NMR (125 MHz, $CDCl_3$) δ 145.8, 143.7, 133.5, 132.1, 131.8, 128.7, 128.1, 127.8, 127.7, 126.6, 79.9, 60.5, 51.8, 40.4, 38.4, 30.6, 24.9, 23.0, 22.6; HRMS (ESI) m/z found $(M + Na)^+$, 391.1434, $C_{23}H_{25}ClO_2$ requires $(M + Na)^+$, 391.1435

(1*R*,2*R*,3*R*)-2-(Hydroxymethyl)-3-(2-methoxyphenyl)-1-phenyl-1,2,3,4,5,6,7,8-octahydronaphthalen-1-ol and (1*S*,2*S*,3*S*)-2-(Hydroxymethyl)-3-(2-methoxyphenyl)-1-phenyl-1,2,3,4,5,6,7,8-octahydronaphthalen-1-ol (12d). White solid, mp 144.7−148.5 °C; R_f 0.3 (1:4, v/v EtOAc/hexanes); IR ν_{max} 3366, 2930, 1599, 1492, 1439, 1241, 1045, 910; ^{1}H NMR (400 MHz, $CDCl_3$) δ 7.48 (br s, 2H), 7.36−7.29 (m, 3H), 7.24−7.19 (m, 2H), 7.01−6.94 (m, 2H), 5.23 (br s, 1H), 4.07 (br s, 1H), 3.89 (s, 3H), 3.38 (t, J = 10.8 Hz, 1H), 3.16−3.12 (m, 2H), 2.63−2.57 (m, 1H), 2.32−2.18 (m, 1H), 2.05 (br s, 2H), 1.91−1.88 (m, 2H), 1.76−1.72 (m, 1H), 1.67−1.62 (m, 1H), 1.50−1.34 (m, 3H); ^{13}C NMR (100 MHz, $CDCl_3$) δ 156.5, 147.2, 132.8, 132.3, 132.0, 131.6, 127.9, 127.5, 126.3, 126.1, 121.9, 111.5, 79.8, 61.9, 56.2, 53.2, 38.5, 30.7, 28.4, 24.9, 23.1, 22.8; HRMS (ESI) m/z found $(M + Na)^+$, 387.1930, $C_{24}H_{28}O_3$ requires $(M + Na)^+$, 387.1931

(1*R*,2*R*,3*R*)-3-(3-Bromophenyl)-2-(hydroxymethyl)-1-phenyl-1,2,3,4,5,6,7,8-octahydronaphthalen-1-ol and (1*S*,2*S*,3*S*)-3-(3-Bromophenyl)-2-(hydroxymethyl)-1-phenyl-1,2,3,4,5,6,7,8-octahydronaphthalen-1-ol (12e). White solid, mp 162.5−163.7 °C; R_f 0.3 (1:9, v/v EtOAc/hexanes); IR ν_{max} 3307, 2928, 1593, 1566, 1474, 1446, 1046, 909, 733; ^{1}H NMR (400 MHz, $CDCl_3$) δ 7.45−7.44 (m, 3H), 7.37−7.33 (m, 3H), 7.27−7.22 (m, 2H), 7.17 (t, J = 7.6 Hz, 1H), 3.45−3.36 (m, 3H), 3.15−3.13 (m, 1H), 2.51 −2.37 (m, 2H), 2.28 (dd, J = 17.6, 5.2, Hz, 1H), 2.04−1.99 (m, 3H), 1.78−1.59 (m, 3H), 1.43−1.39 (m, 3H), ^{13}C NMR (100 MHz, $CDCl_3$) δ 146.6, 145.8, 133.0, 132.2, 130.8, 130.1, 129.6, 128.0, 126.9, 126.5, 126.2, 122.6, 80.1, 60.4, 51.8, 40.3, 38.2, 30.6, 24.9, 23.1, 22.6; HRMS (ESI) m/z found $(M + Na)^+$, 435.0924, $C_{23}H_{25}BrO_2$ requires $(M + Na)^+$, 435.0930

(1*R*,2*R*,3*R*)-3-(2-Bromocyclohex-1-en-2-yl)-2-(hydroxymethyl)-1-phenyl-1,2,3,4,5,6,7,8-octahydronaphthalen-1-ol and (1*S*,2*S*,3*S*)-3-(2-Bromocyclohex-1-en-2-yl)-2-(hydroxymethyl)-1-phenyl-1,2,3,4,5,6,7,8-octahydronaphthalen-1-ol (12f). White solid, mp 106.4−110.3 °C; R_f 0.3 (1:9, v/v EtOAc/hexanes); IR ν_{max} 3369, 2931, 1446, 1333, 1046, 966, 909, 733; ^{1}H NMR (400 MHz, $CDCl_3$) δ 7.43−7.41 (m, 2H), 7.33 (t, J = 7.2 Hz, 2H), 7.24−7.20 (m, 1H), 4.10 (s, 1H), 3.74 (td, J = 12.0, 5.2 Hz, 1H), 3.48−3.46 (m, 2H), 2.59−2.58 (m, 2H), 2.25−2.15 (m, 3H), 2.04−1.81 (m, 5H), 1.78−1.67 (m, 5H), 1.63−1.56 (m, 2H), 1.41−1.26 (m, 3H); ^{13}C NMR (100 MHz, $CDCl_3$) δ 146.5, 136.5, 132.3, 131.8, 127.9, 126.3, 126.2, 121.4, 79.2, 62.1, 49.0, 38.6, 37.2, 34.3, 30.7, 26.5, 24.9, 23.0, 22.7, 22.5 one signal overlapping or missing; HRMS (ESI) m/z found $(M + Na)^+$, 439.1239, $C_{23}H_{29}BrO_2$ requires $(M + Na)^+$, 439.1243

(1*R*,2*R*,3*R*,4*R*)-2-(Hydroxymethyl)-4-methyl-1,3-diphenyl-1,2,3,4,5,6,7,8-octahydronaphthalen-1-ol and (1*S*,2*S*,3*S*,4*S*)-2-(Hydroxymethyl)-4-methyl-1,3-diphenyl-1,2,3,4,5,6,7,8-octahydronaphthalen-1-ol (12g). White solid, mp 164.9−167.7 °C; R_f 0.3 (1:4, v/v EtOAc/hexanes); IR ν_{max} 3305, 2929, 1446, 1059, 1029, 910; ^{1}H NMR (300 MHz, $CDCl_3$) δ 7.48 (d, J = 7.5 Hz, 2H), 7.38−7.22 (m, 8H), 3.49 (s, 1H), 3.32 (ddd, J = 11.7, 3.6, 1.5 Hz, 1H), 3.10−2.99 (m, 2H), 2.58−2.46 (m, 1H), 2.27 (dd, J = 7.5, 3.6 Hz, 1H), 2.25−2.18 (m, 1H), 2.10 (dq, J = 12.3, 1.8 Hz, 1H), 2.00−1.93 (m, 1H), 1.82−1.77 (m, 2H), 1.71−1.68 (m, 1H), 1.50−1.25 (m, 3H), 0.95 (d, J = 6.9 Hz, 3H); ^{13}C NMR (75 MHz, $CDCl_3$) δ 146.3, 143.6, 137.1, 132.2, 128.5, 128.0, 126.4, 126.3(2), 126.2(7), 79.7, 61.3, 51.2, 46.0, 42.3, 28.6, 25.9, 22.9, 17.3 two signals overlapping or missing; HRMS (ESI) m/z found $(M + Na)^+$, 371.1986, $C_{24}H_{28}O_2$ requires $(M + Na)^+$, 371.1982

(1*R*,2*R*,3*R*,4*R*)-4-Allyl-2-(Hydroxymethyl)-1,3-diphenyl-1,2,3,4,5,6,7,8-octahydronaphthalen-1-ol and (1*S*,2*S*,3*S*,4*S*)-4-Allyl-2-(Hydroxymethyl)-1,3-diphenyl-1,2,3,4,5,6,7,8-octahydronaphthalen-1-ol (12h). White solid, mp 149.5−150.5 °C; R_f 0.3 (1:4, v/v EtOAc/hexanes); IR ν_{max} 3338, 2927, 1491, 1446, 1045, 909; ^{1}H NMR (400 MHz, $CDCl_3$) δ 7.38−7.29 (m, 8H), 7.25−7.21 (m, 2H), 5.82−5.72 (m, 1H), 5.16−5.07 (m, 2H), 3.36 (dd, J = 12.4, 10.4 Hz, 1H), 3.26 (dd, J = 10.4, 2.0 Hz, 1H), 3.03 (s, 1H), 2.96 (ddd, J = 12.4, 8.0, 3.2 Hz, 1H), 2.63−2.60 (m, 1H), 2.49−2.43 (m, 1H), 2.33 (dd, J = 8.0, 3.2 Hz, 1H), 2.29−2.25 (m, 1H), 2.10−1.92 (m, 3H), 1.83−1.65 (m, 3H), 1.49−1.42 (m, 1H), 1.35−1.25 (m, 3H); ^{13}C NMR (100 MHz, $CDCl_3$) δ 145.7, 143.3, 135.0, 134.8, 134.6, 128.6, 128.0, 126.5, 126.4, 126.3, 126.2, 117.9, 79.4, 61.4, 50.7, 46.1, 40.7, 32.5, 28.6, 26.4, 23.0, 22.9; HRMS (ESI) m/z found $(M + Na)^+$, 397.2135, $C_{26}H_{30}O_2$ requires $(M + Na)^+$, 397.2138

(1*R*,2*R*,3*R*)-2-(Hydroxymethyl)-1,3-diphenyl-2,3,4,5,6,7,8,9-octahydro-1*H*-benzo[7]annulen-1-ol and (1*S*,2*S*,3*S*)-2-(Hydroxymethyl)-1,3-diphenyl-2,3,4,5,6,7,8,9-octahydro-1*H*-benzo[7]-annulen-1-ol (12i). Clear oil; R_f 0.3 (1:4, v/v EtOAc/hexanes); IR ν_{max} 3332, 2921, 1493, 1446, 1036, 909; ^{1}H NMR (500 MHz, $CDCl_3$) δ 7.46 (br s, 2H), 7.38−7.31 (m, 6H), 7.25−7.20 (m, 2H), 3.41 (d, J = 12.0 Hz, 1H), 3.33 (td, J = 12.0, 5.0 Hz, 1H), 3.28 (s, 1H), 3.15 (ddd, J = 11.0, 7.5, 3.0 Hz, 1H), 2.58 (dd, J = 18.0, 11.0 Hz, 1H), 2.46−2.45 (m, 1H), 2.40 (dd, J = 18.0, 5.0 Hz, 1H), 2.20−2.05 (m, 2H), 1.96 (dm, J = 12.0 Hz, 1H), 1.86−1.82 (m, 1H), 1.75−1.48 (m, 5H), 1.38−1.24 (m, 2H); ^{13}C NMR (125 MHz, $CDCl_3$) δ 146.2, 143.9, 139.3, 137.2, 128.6, 127.9, 126.5, 126.4, 126.2, 81.8, 60.5, 51.9, 42.2, 39.0, 35.4, 32.3, 30.2, 26.7, 25.9 one signal overlapping or missing; HRMS (ESI) m/z found $(M + Na)^+$, 371.1984, $C_{24}H_{28}O_2$ requires $(M + Na)^+$, 371.1982

General Procedure for the NHC-Catalyzed (4 + 2) Cycloaddition/Carbanion Addition. A solution of IPrMe (0.1 M in THF, 0.2 mL, 0.02 mmol) was added to a stirred solution of TMS ether **1** (0.2 mmol) and acid fluoride **2** (0.2 mmol) in THF (3 mL) at −78 °C. The reaction mixture was allowed to warm to −20 °C over the period of one hour, and maintained between −20 and −30 °C for an additional hour. The reaction was then recooled to −78 °C and the appropriate organolithium reagent (0.4 mmol) added. The reaction mixture was allowed to warm to −10 °C, after which time it was quenched with water. The aqueous layer was extracted with ethyl acetate (3 × 10 mL) and the combined organic layers were dried ($MgSO_4$), filtered and evaporated. The crude residue was purified *via* flash column chromatography (1:10 or 1:20 v/v EtOAc/hexanes) to provide the pure ketone illustrated below.

1-((1*R*,2*S*,3*R*)-1-Hydroxy-1,3-diphenyl-1,2,3,4,5,6,7,8-octahydronaphthalen-2-yl)ethanone and 1-((1*S*,2*R*,3*S*)-1-Hydroxy-1,3-diphenyl-1,2,3,4,5,6,7,8-octahydronaphthalen-2-yl)-ethanone (13a). White solid, mp 153.8−155.8 °C; R_f 0.3 (1:9, v/v EtOAc/hexanes); IR ν_{max} 3429, 2929, 1693, 1492, 1447, 1356, 1167, 1043; ^{1}H NMR (400 MHz, $CDCl_3$) δ 7.34−7.20 (m, 10H), 4.84 (s, 1H), 3.54 (td, J = 12.0, 5.2 Hz, 1H), 3.50 (d, J = 12.0 Hz, 1H), 2.57−2.47 (m, 1H), 2.35−2.29 (m, 1H), 2.06 (br s, 2H), 1.87−1.63 (m, 3H), 1.52−1.45 (m, 3H), 1.22 (s, 3H); ^{13}C NMR (100 MHz, $CDCl_3$) δ 216.1, 145.4, 142.5, 132.1, 131.5, 128.6, 128.2, 127.9, 126.9, 126.7, 126.0, 76.5, 64.4, 40.3, 39.1, 34.3, 30.6, 25.0, 23.0, 22.7; HRMS (ESI) m/z found $(M + Na)^+$, 369.1819, $C_{24}H_{26}O_2$ requires $(M + Na)^+$, 369.1825

1-((1*R*,2*S*,3*R*)-1-Hydroxy-1,3-diphenyl-1,2,3,4,5,6,7,8-octahydronaphthalen-2-yl)pentan-1-one and 1-((1*S*,2*R*,3*S*)-1-Hydroxy-1,3-diphenyl-1,2,3,4,5,6,7,8-octahydronaphthalen-2-yl)-pentan-1-one (13b). White solid, mp 138.6−141.0 °C; R_f 0.3 (1:19, v/v EtOAc/hexanes); IR ν_{max} 3454, 2931, 1684, 1601, 1493, 1453, 1367, 1126, 1049; ^{1}H NMR (300 MHz, $CDCl_3$) δ 7.29−7.17 (m, 10H), 5.15 (s, 1H), 3.57 (td, J = 12.0, 5.4 Hz, 1H), 3.38 (d, J = 12.0 Hz, 1H), 2.59−2.50 (m, 1H), 2.32 (dd, J = 17.7, 4.8 Hz, 1H), 2.06 (br s, 2H), 1.87−1.67 (m, 3H), 1.52−1.38 (m, 4H), 1.31−1.20 (m, 1H), 0.81−0.55 (m, 4H), 0.48 (t, J = 6.3 Hz, 3H); ^{13}C NMR (100 MHz, $CDCl_3$) δ 218.3, 145.5, 142.3, 132.0, 131.5, 128.5, 128.1, 128.0, 126.9, 126.6, 126.0, 76.6, 64.3, 46.7, 40.4, 38.8, 30.6, 25.0, 23.8, 23.0, 22.7,

dx.doi.org/10.1021/jo202500k | *J. Org. Chem.* 2012, 77, 1113−1124

21.3, 13.4; HRMS (ESI) m/z found $(M + Na)^+$, 411.2289, $C_{27}H_{32}O_2$ requires $(M + Na)^+$, 411.2295

1-((1*R*,2*S*,3*R*)-1-Hydroxy-1,3-diphenyl-1,2,3,4,5,6,7,8-octahydronaphthalen-2-yl)-3-methylbutan-1-one and 1-((1*S*,2*R*,3*S*)-1-Hydroxy-1,3-diphenyl-1,2,3,4,5,6,7,8-octahydronaphthalen-2-yl)-3-methylbutan-1-one (13c). White solid, mp 157.1−160.2 °C; R_f 0.3 (1:19, v/v EtOAc/hexanes); IR ν_{max} 3461, 2928, 1682, 1493, 1446, 1366, 1049; ^{1}H NMR (300 MHz, $CDCl_3$) δ 7.38−7.16 (m, 10H), 5.15 (s, 1H), 3.56 (td, J = 12.0, 5.2 Hz, 1H), 3.33 (d, J = 12.0 Hz, 1H), 2.57−2.50 (m, 1H), 2.32 (dd, J = 17.6, 4.4 Hz, 1H), 2.05 (br s, 2H), 1.85−1.65 (m, 3H), 1.50−1.39 (m, 4H), 1.31 (dd, J = 18.8, 6.8 Hz, 1H), 1.13 (dd, J = 18.8, 6.8 Hz, 1H), 0.29 (d, J = 6.8 Hz, 3H), 0.16 (d, J = 6.8 Hz, 3H); ^{13}C NMR (100 MHz, $CDCl_3$) δ 217.6, 145.4, 142.3, 132.0, 131.5, 128.5, 128.1, 128.0, 126.9, 126.6, 126.1, 76.6, 64.1, 56.2, 40.4, 28.9, 30.6, 25.0, 23.0, 22.7, 22.0, 21.9, 21.4; HRMS (ESI) m/z found $(M + Na)^+$, 411.2292, $C_{27}H_{32}O_2$ requires $(M + Na)^+$, 411.2295

1-((1*R*,2*S*,3*R*)-1-Hydroxy-1,3-diphenyl-1,2,3,4,5,6,7,8-octahydronaphthalen-2-yl)-2-methylbutan-1-one and 1-((1*S*,2*R*,3*S*)-1-Hydroxy-1,3-diphenyl-1,2,3,4,5,6,7,8-octahydronaphthalen-2-yl)-2-methylbutan-1-one (13d). White solid, mp 147.2−150.0 °C; R_f 0.3 (1:19, v/v EtOAc/hexanes); IR ν_{max} 3433, 2930, 1675, 1600, 1493, 1453, 1370, 1051; ^{1}H NMR (300 MHz, $CDCl_3$) δ 7.35 (t, J = 7.2 Hz, 2H), 7.31−7.25 (m, 6H), 7.21−7.16 (m, 2H), 5.73 (s, 0.5H), 5.69 (s, 0.5H), 3.61−3.53 (m, 1H), 3.41 (d, J = 11.6 Hz, 0.5H), 3.40 (d, J = 11.6 Hz, 0.5H), 2.67−2.56 (m, 1H), 2.30 (dd, J = 17.6, 2.8 Hz, 1H), 2.06 (br s, 2H), 1.84−1.73 (m, 2H), 1.68−1.64 (m, 1H), 1.49−1.29 (m, 4H), 0.60−0.35 (m, 2H), 0.23 (t, J = 6.8 Hz, 1.5H), 0.14 (t, J = 7.6 Hz, 1.5 H), 0.00 (d, J = 6.8 Hz, 1.5H), −0.06 (d, J = 6.8 Hz, 1.5H); ^{13}C NMR (100 MHz, $CDCl_3$) δ 222.2, 221.8, 145.9, 142.0, 141.0, 132.0, 131.0, 131.8(8), 131.8(1), 128.5(4), 128.5(1), 128.4, 128.0, 127.1, 127.0, 126.6(4), 126.6(3), 77.2, 63.9, 63.5, 50.7, 50.3, 41.3(2), 41.3(0), 38.9, 38.5, 30.7, 30.6, 25.1, 25.0, 23.1, 22.9, 22.7, 22.5, 12.7, 12.0, 10.4(9), 10.4(5) eight signals overlapping or missing; HRMS (ESI) m/z found $(M + Na)^+$, 411.2292, $C_{27}H_{32}O_2$ requires $(M + Na)^+$, 411.2295

1-((1*R*,2*S*,3*R*)-1-Hydroxy-1,3-diphenyl-1,2,3,4,5,6,7,8-octahydronaphthalen-2-yl)-2,2-dimethylpropan-1-one and 1-((1*S*,2*R*,3*S*)-1-Hydroxy-1,3-diphenyl-1,2,3,4,5,6,7,8-octahydronaphthalen-2-yl)-2,2-dimethylpropan-1-one (13e). White solid, mp 187.4−190.3 °C; R_f 0.3 (1:19, v/v EtOAc/hexanes); IR ν_{max} 3448, 2913, 1735, 1675, 1657, 1444, 1364, 1259, 1051; ^{1}H NMR (500 MHz, $CDCl_3$) δ 7.38−7.37 (m, 2H), 7.30 (t, J = 7.5 Hz, 2H), 7.26−7.25 (m, 4H), 7.21−7.18 (m, 2H), 5.52 (s, 1H), 3.87 (d, J = 12.0 Hz, 1H), 3.59 (td, J = 12.0, 5.0 Hz, 1H), 2.66 (dd, J = 17.5, 14.0 Hz, 1H), 2.30 (dd, J = 17.5, 5.0 Hz, 1H), 2.07 (br s, 2H), 1.79−1.64 (m, 3H), 1.47−1.39 (m, 3H), 0.12 (s, 9H); ^{13}C NMR (125 MHz, $CDCl_3$) δ 225.8, 145.8, 142.3, 131.9, 131.8, 129.0, 128.4, 128.1, 127.1, 126.8, 126.6, 77.0, 59.4, 44.2, 41.2, 37.9, 30.6, 26.1, 25.3, 23.1, 22.7; HRMS (ESI) m/z found $(M + Na)^+$, 411.2291, $C_{27}H_{32}O_2$ requires $(M + Na)^+$, 411.2295

((1*R*,2*S*,3*R*)-1-Hydroxy-1,3-diphenyl-1,2,3,4,5,6,7,8-octahydronaphthalen-2-yl)(phenyl)methanone and ((1*S*,2*R*,3*S*)-1-Hydroxy-1,3-diphenyl-1,2,3,4,5,6,7,8-octahydronaphthalen-2-yl)(phenyl)methanone (13f). White solid, mp 196.3−199.8 °C; R_f 0.3 (1:9, v/v EtOAc/hexanes); IR ν_{max} 3448, 2935, 2915, 1643, 1447, 1355, 1223, 908; ^{1}H NMR (400 MHz, $CDCl_3$) δ 7.45−7.38 (m, 3H), 7.23−7.18 (m, 3H), 7.11−7.06 (m, 3H), 7.02−6.94 (m, 6H), 5.37 (s, 1H), 4.25 (d, J = 12.0 Hz, 1H), 3.70 (td, J = 12.0, 5.2 Hz, 1H), 2.61−2.53 (m, 1H), 2.36 (dd, J = 17.6, 5.2 Hz, 1H), 2.10 (br s, 2H), 1.93−1.89 (m, 1H), 1.82−1.77 (m, 1H), 1.72−1.67 (m, 1H), 1.62−1.50 (m, 3H); ^{13}C NMR (100 MHz, $CDCl_3$) δ 208.1, 145.7, 141.8, 138.9, 132.3, 132.0, 129.8, 128.2, 128.0, 127.7, 127.4, 126.9, 126.6, 126.5, 126.1, 77.2, 59.2, 41.6, 39.6, 30.8, 25.1, 23.1, 22.8; HRMS (ESI) m/z found $(M + Na)^+$, 431.1981, $C_{29}H_{28}O_2$ requires $(M + Na)^+$, 431.1982

((1*R*,2*S*,3*R*)-1-Hydroxy-1,3-diphenyl-1,2,3,4,5,6,7,8-octahydronaphthalen-2-yl)(4-methoxyphenyl)methanone and ((1*S*,2*R*,3*S*)-1-Hydroxy-1,3-diphenyl-1,2,3,4,5,6,7,8-octahydronaphthalen-2-yl)(4-methoxyphenyl)methanone (13g). White solid, mp 191.8−194.3 °C; R_f 0.3 (1:9, v/v EtOAc/hexanes); IR ν_{max} 3435, 2930, 1634, 1599, 1571, 1493, 1453, 1352, 1263, 1228, 1175, 1026; ^{1}H NMR (400 MHz, $CDCl_3$) δ 7.39−7.37 (m, 2H), 7.19 (t, J = 8.0 Hz, 2H), 7.13−7.19 (m, 4H), 7.07−6.93 (m, 4H), 6.51−6.48 (m, 2H), 5.52 (s, 1H), 4.20 (d, J = 11.6 Hz, 1H), 3.70 (s, 3H), 3.73−3.67 (m, 1H), 2.59−2.52 (m, 1H), 2.36 (dd, J = 17.6, 4.4 Hz, 1H), 2.10 (br s, 2H), 1.93−1.89 (m, 1H), 1.81−1.78 (m, 1H), 1.72−1.68 (m, 1H), 1.59−1.48 (m, 3H); ^{13}C NMR (100 MHz, $CDCl_3$) δ 205.7, 163.1, 145.9, 142.1, 132.2, 132.1, 131.7, 130.0, 128.0, 127.9(8), 127.9(7), 126.4(6), 126.4(5), 126.1, 112.9, 77.1, 58.2, 55.2, 41.4, 39.6, 30.7, 25.2, 23.1, 22.8; HRMS (ESI) m/z found $(M + Na)^+$, 461.2091, $C_{30}H_{30}O_3$ requires $(M + Na)^+$, 461.2087

1-((1*R*,2*S*,3*R*)-1-(4-Chlorophenyl)-1-hydroxy-3-phenyl-1,2,3,4,5,6,7,8-octahydronaphthalen-2-yl)pentan-1-one and 1-((1*S*,2*R*,3*S*)-1-(4-Chlorophenyl)-1-hydroxy-3-phenyl-1,2,3,4,5,6,7,8-octahydronaphthalen-2-yl)pentan-1-one (13h). White solid, mp 148.3−150.3 °C; R_f 0.3 (1:19, v/v EtOAc/hexanes); IR ν_{max} 3443, 2930, 1687, 1601, 1488, 1453, 1396, 1092; ^{1}H NMR (400 MHz, $CDCl_3$) δ 7.29−7.16 (m, 9H), 5.23 (s, 1H), 3.51 (td, J = 11.6, 5.2 Hz, 1H), 3.28 (d, J = 11.6 Hz, 1H), 2.54−2.46 (m, 1H), 2.28 (dd, J = 17.2, 4.4 Hz, 1H), 2.01 (br s, 2H), 1.79−1.61 (m, 3H), 1.45−1.24 (m, 5H), 0.79−0.67 (m, 2H), 0.61−0.55 (m, 2H), 0.46 (t, J = 6.4 Hz, 3H); ^{13}C NMR (100 MHz, $CDCl_3$) δ 218.1, 144.2, 142.0, 132.5, 132.4, 131.1, 128.6, 128.2, 128.0, 127.6, 127.0, 76.4, 64.0, 46.7, 40.5, 38.6, 30.6, 25.0, 23.9, 23.0, 22.6, 21.3 13.4; HRMS (ESI) m/z found $(M + Na)^+$, 445.1908, $C_{27}H_{31}ClO_2$ requires $(M + Na)^+$, 445.1905

1-((1*R*,2*S*,3*R*)-3-(3-Bromophenyl)-1-hydroxy-1-phenyl-1,2,3,4,5,6,7,8-octahydronaphthalen-2-yl)ethanone and 1-((1*S*,2*R*,3*S*)-3-(3-Bromophenyl)-1-hydroxy-1-phenyl-1,2,3,4,5,6,7,8-octahydronaphthalen-2-yl)ethanone (13i). Clear oil R_f 0.3 (1:9, v/v EtOAc/hexanes); IR ν_{max} 3435, 2929, 1694, 1594, 1566, 1475, 1446, 1357; ^{1}H NMR (300 MHz, $CDCl_3$) δ 7.44−7.32 (m, 6H), 7.27−7.24 (1H), 7.18−7.15 (m, 2H), 4.61 (s, 1H), 3.53 (td, J = 12.0, 5.1 Hz, 1H), 3.47 (d, J = 12.0 Hz, 1H), 2.49−2.40 (m, 1H), 2.33−2.26 (m, 1H), 2.04 (br s, 2H), 1.85−1.61 (m, 3H), 1.52−1.42 (m, 3H), 1.27 (s, 3H); ^{13}C NMR (100 MHz, $CDCl_3$) δ 215.4, 145.1, 145.0, 131.9, 131.7, 130.6, 130.2, 130.1, 128.2, 126.7, 125.9, 122.7, 76.4, 64.2, 40.0, 39.1, 34.3, 30.6, 35.0, 23.0, 22.6 one signal missing or overlapping; HRMS (ESI) m/z found $(M + Na)^+$, 447.0920, $C_{24}H_{25}BrO_2$ requires $(M + Na)^+$, 447.0930

1-((1*R*,2*S*,3*R*)-1-Hydroxy-1,3-diphenyl-2,3,4,5,6,7,8,9-octahydro-1*H*-benzo[7]annulen-2-yl)ethanone and 1-((1*S*,2*R*,3*S*)-1-Hydroxy-1,3-diphenyl-2,3,4,5,6,7,8,9-octahydro-1*H*-benzo[7]annulen-2-yl)ethanone (13j). White solid, mp 95.6−99.5 °C; R_f 0.3 (1:9, v/v EtOAc/hexanes); IR ν_{max} 3434, 2922, 1694, 1492, 1447, 1356, 1256; ^{1}H NMR (500 MHz, $CDCl_3$) δ 7.39−7.19 (m, 10H), 4.77 (s, 1H), 3.47 (td, J = 12.0, 5.5 Hz, 1H), 3.40 (d, J = 12.0 Hz, 1H), 2.63 (dd, J = 18.0, 11.0 Hz, 1H), 2.41 (dd, J = 18.0, 5.0 Hz, 1H), 2.29−2.18 (m, 3H), 1.92−1.90 (m, 2H), 1.75−1.51 (m, 3H), 1.38−1.34 (m, 2H), 1.19 (s, 3H); ^{13}C NMR (100 MHz, $CDCl_3$) δ 216.0, 145.7, 142.5, 138.0, 136.6, 128.6, 128.1, 127.8, 126.9, 126.7, 125.8, 78.1, 64.4, 40.9, 40.7, 35.2, 34.2, 32.2, 30.2, 27.3, 25.9; HRMS (ESI) m/z found $(M + Na)^+$, 383.1984, $C_{25}H_{28}O_2$ requires $(M + Na)^+$, 383.1982

1-((1*R*,2*S*,3*R*,4*R*)-1-Hydroxy-4-methyl-1,3-diphenyl-1,2,3,4,5,6,7,8-octahydronaphthalen-2-yl)pentan-1-one and 1-((1*S*,2*R*,3*S*,4*S*)-1-Hydroxy-4-methyl-1,3-diphenyl-1,2,3,4,5,6,7,8-octahydronaphthalen-2-yl)pentan-1-one (13k). White solid, mp 128.9−130.8 °C; R_f 0.3 (1:19, v/v EtOAc/hexanes); IR ν_{max} 3454, 2929, 1682, 1492, 1445, 1374, 1261, 1054, 1030; ^{1}H NMR (300 MHz, $CDCl_3$) δ 7.39−7.17 (m, 10H), 5.10 (s, 1H), 3.42 (d, J = 12.4 Hz, 1H), 3.16 (dd, J = 12.4, 10.4 Hz, 1H), 2.57 (br s, 1H), 2.26−2.22 (m, 1H), 1.96−1.92 (m, 1H), 1.83−1.78 (m, 2H), 1.71−1.64 (m, 1H), 1.55−1.49 (m, 1H), 1.42−1.23 (m, 5H), 0.96−0.94 (m, 2H), 0.89−0.50 (m, 4H), 0.45 (t, J = 6.4 Hz, 3H); ^{13}C NMR (100 MHz, $CDCl_3$) δ 218.5, 145.6, 141.9, 136.1, 131.4, 128.9, 128.5, 128.2, 126.8, 126.5, 126.1, 76.0, 63.6, 47.8, 46.5, 41.4, 28.6, 25.9, 23.8, 22.8, 21.3, 16.6, 13.5, 1.0; HRMS (ESI) m/z found $(M + Na)^+$, 425.2452, $C_{28}H_{34}O_2$ requires $(M + Na)^+$, 425.2451

■ ASSOCIATED CONTENT

Ⓢ Supporting Information

Details of computation methods used, Cartesian coordinates and energies of optimized geometries, complete reference 15,

dx.doi.org/10.1021/jo202500k | J. Org. Chem. 2012, 77, 1113−1124

together with characterization data, NMR spectra, and crystallographic data in CIF format. This material is available free of charge via the Internet at http://pubs.acs.org.

AUTHOR INFORMATION

Corresponding Author

*E-mail: m.paddonrow@unsw.edu.au; david.lupton@monash.edu.

ACKNOWLEDGMENTS

We acknowledge financial support from the Australian Research Council (DP0881137; DP120101315) and Monash University (Research Accelerator Program). We thank the NCI National Facility for computer time, awarded under the Merit Allocation Scheme. Part of this research was undertaken on the MX1 beamline at the Australian Synchrotron, Victoria, Australia.

REFERENCES

(1) For reviews on NHC organocatalysis, see: (a) Zeitler, K. *Angew. Chem., Int. Ed.* **2005**, *44*, 7506. (b) Enders, D.; Niemeier, O.; Henseler, A. *Chem. Rev.* **2007**, *107*, 5606. (c) Marion, N.; Díez-González, S.; Nolan, S. P. *Angew. Chem., Int. Ed.* **2007**, *46*, 2988. (d) Moore, J. L.; Rovis, T. *Top. Curr. Chem.* **2009**, *290*, 77. (e) Phillips, E. M.; Chan, A.; Scheidt, K. A. *Aldrichimica Acta* **2009**, *42*, 55. (f) Vora, H. U.; Rovis, T. *Aldrichimica Acta* **2011**, *44*, 3. (g) Chiang, P.-C.; Bode, J. W. *TCIMail* **2011**, *149*, 2. (h) Nair, V.; Menon, R. S.; Biju, A. T.; Sinu, C. R.; Paul, R. R.; Jose, A.; Sreekumar, V. *Chem. Soc. Rev.* **2011**, *40*, 5336.

(2) For reviews on recent studies on NHC-acyl anion catalysis, see: (a) Johnson, J. S. *Angew. Chem., Int. Ed.* **2004**, *43*, 1326. (b) Biju, A. T.; Kuhl, N.; Glorius, F. *Acc. Chem. Res.* **2011**, *44*, 1182−1195.

(3) For leading examples of NHC-acyl azolium catalysis, see: (a) Chow, K. Y.-K.; Bode, J. W. *J. Am. Chem. Soc.* **2004**, *126*, 8126. (b) Reynolds, N. T.; Read de Alaniz, J.; Rovis, T. *J. Am. Chem. Soc.* **2004**, *126*, 9518. (c) Burstein, C.; Glorius, F. *Angew. Chem., Int. Ed.* **2004**, *43*, 6205. (d) Sohn, S. S.; Rosen, E. L.; Bode, J. W. J. *Am. Chem. Soc.* **2004**, *126*, 14370. (e) Chan, A.; Scheidt, K. A. *Org. Lett.* **2005**, *7*, 905. (f) Zeitler, K. *Org. Lett.* **2006**, *8*, 637.

(4) For leading examples of NHC-Brønsted base catalysis, see: (a) Grasa, G. A.; Kissling, R. M.; Nolan, S. P. *Org. Lett.* **2002**, *4*, 3583. (b) Nyce, G. W.; Lamboy, J. A.; Connor, E. F.; Waymouth, R. M.; Hedrick, J. L. *Org. Lett.* **2002**, *4*, 3587. (c) Nyce, G. W.; Glauser, T.; Connor, E. F.; Möck, A.; Waymouth, R. M.; Hedrick, J. L. *J. Am. Chem. Soc.* **2003**, *125*, 3046. (d) Grasa, G. A.; Singh, R.; Nolan, S. P. *Synthesis* **2004**, 971.

(5) For NHC-Lewis base activation at the carbonyl group without acyl anion formation, see: (a) Ryan, S. J.; Candish, L.; Lupton, D. W. *J. Am. Chem. Soc.* **2009**, *131*, 14176. (b) Candish, L.; Lupton, D. W. *Org. Lett.* **2010**, *12*, 4836. (c) Candish, L.; Lupton, D. W. *Org. Biomol. Chem.* **2011**, *9*, 8182. (d) Ryan, S. J.; Candish, L.; Lupton, D. W. *J. Am. Chem. Soc.* **2011**, *133*, 4694. (e) Candish, L.; Lupton, D. W. *Chem. Sci.* **2012**, DOI: 10.1039/C1SC00666E. (f) Ryan, S. J.; Candish, L.; Lupton, D. W. *Synlett* **2011**, 2275.

(6) For examples of NHC-Lewis base activation by conjugate addition, see: (a) Fischer, C.; Smith, S. W.; Powell, D. A.; Fu, G. C. *J. Am. Chem. Soc.* **2006**, *128*, 1472. (b) Matsuoka, S.-i.; Ota, Y.; Washio, A.; Katada, A.; Ichioka, K.; Takagi, K.; Suzuki, M. *Org. Lett.* **2011**, *13*, 3722. (c) Biju, A. T.; Padmanaban, M.; Wurz, N. E.; Glorius, F. *Angew. Chem., Int. Ed.* **2011**, *50*, 8412. (d) Atienza, R. L.; Roth, H. S.; Scheidt, K. A. *Chem. Sci.* **2011**, *2*, 1772. (e) Atienza, R. L.; Scheidt, K. A. *Aust. J. Chem.* **2011**, *64*, 1158.

(7) For selected examples of cooperative NHC catalysis, see: (a) Lebeuf, R.; Hirano, K.; Glorius, F. *Org. Lett.* **2008**, *10*, 4243. (b) Raup, D. E. A.; Cardinal-David, B.; Holte, D.; Scheidt, K. A. *Nat. Chem.* **2010**, *2*, 766. (c) Cardinal-David, B.; Raup, D. E. A.; Scheidt, K. A. *J. Am. Chem. Soc.* **2010**, *132*, 5345. (d) Cohen, D. T.; Cardinal-David, B.; Scheidt, K. A. *Angew. Chem., Int. Ed.* **2011**, *50*, 1678. (e) Ozboya, K. E.; Rovis, T. *Chem. Sci.* **2011**, *2*, 1835. (f) Lathrop, S. P.; Rovis, T. *J. Am. Chem. Soc.* **2009**, *131*, 13628. (g) Vora, H. U.; Rovis, T. *J. Am. Chem. Soc.* **2007**, *129*, 13796. (h) Padmanaban, M.; Biju, A. T.; Glorius, F. *Org. Lett.* **2011**, *13*, 5624. For a recent review on dual activation, see: (i) Hirano, K.; Piel, I.; Glorius, F. *Chem. Lett.* **2011**, *40*, 786.

(8) For reviews focused on the properties of NHCs, see: (a) Dröge, T.; Glorius, F. *Angew. Chem., Int. Ed.* **2010**, *49*, 6940. (b) Maji, B.; Breugst, M.; Mayr, H. *Angew. Chem., Int. Ed.* **2011**, *50*, 6915. For discussion of the role of the electronics of the *N*-aryl group in triazolium based NHC-catalysis, see: (c) Rovis, T. *Chem. Lett.* **2008**, *37*, 2. (d) Mahatthananchai, J.; Bode, J. W. *Chem. Sci.* **2011**, DOI: 10.1039/C1SC00397F.

(9) For a recent review on quantum mechanics in organocatalysis, see: (a) Cheong, P. H.-Y.; Legault, C. Y.; Um, J. M.; Içüm, N. C.; Houk, K N. *Chem. Rev.* **2011**, *111*, 5042. For selected examples of computational studies on NHC catalysis, see: (b) Um, J. M.; DiRocco, D. A.; Noey, E. L.; Rovis, T.; Houk, K. N. *J. Am. Chem. Soc.* **2011**, *133*, 11249. (c) Hawkes, K. J.; Yates, B. F. *Eur. J. Org. Chem.* **2008**, 5563. (d) Gonzalez-James, O. M.; Singleton, D. A. *J. Am. Chem. Soc.* **2010**, *132*, 6896. For acyl azolium catalysis, see: (e) Domingo, L. R.; Zaragozá, R. J.; Arnó, M. *Org. Biomol. Chem.* **2010**, *8*, 4884. (f) Domingo, L. R.; Zaragozá, R. J.; Arnó, M. *Org. Biomol. Chem.* **2011**, *9*, 6616. (g) Verma, P.; Patni, P. A.; Sunoj, R. B. *J. Org. Chem.* **2011**, *76*, 5606.

(10) For NHC-catalyzed hetero Diels−Alder reactions, see: (a) He, M.; Struble, J. R.; Bode, J. W. *J. Am. Chem. Soc.* **2006**, *128*, 8418. (b) He, M.; Uc, G. J.; Bode, J. W. *J. Am. Chem. Soc.* **2006**, *128*, 15088. (c) He, M. H.; Beahm, B. J.; Bode, J. W. *Org. Lett.* **2008**, *10*, 3817. (d) Kaeobamrung, J.; Kozlowski, M. C.; Bode, J. W. *Proc. Nat. Acad. Sci. U.S.A.* **2010**, *107*, 20661.

(11) For a review on Diels−Alder mechanistic studies, see: (a) Houk, K. N.; González, J.; Li, Y. *Acc. Chem. Res.* **1995**, *28*, 81. For reviews covering the Diels−Alder reaction, in catalysis: (b) Corey, E. J. *Angew. Chem., Int. Ed.* **2002**, *41*, 1650. In total synthesis: (c) Juhl, M.; Tanner, D. *Chem. Soc. Rev.* **2009**, *38*, 2983. (d) Nicolaou, K. C.; Snyder, S. A.; Montagnon, T.; Vassilikogiannakis, G. *Angew. Chem., Int. Ed.* **2002**, *41*, 1668.

(12) For NHC-catalyzed reactions involving *β*-lactones, see: (a) Burstein, C.; Tschan, S.; Xie, X.; Glorius, F. *Synthesis* **2006**, 2418. (b) Nair, V.; Vellalath, S.; Poonoth, M.; Suresh, E. *J. Am. Chem. Soc.* **2006**, *128*, 8736. (c) Chiang, P.-C.; Kaeobamrung, J.; Bode, J. W. *J. Am. Chem. Soc.* **2007**, *129*, 3520. (d) Wadamoto, M.; Phillips, E. M.; Reynolds, T. E.; Scheidt, K. A. *J. Am. Chem. Soc.* **2007**, *129*, 10098. (e) He, M.; Bode, J. W. *J. Am. Chem. Soc.* **2008**, *130*, 418. (f) Kaeobamrung, J.; Bode, J. W. *Org. Lett.* **2009**, *11*, 677. (g) Phillips, E. M.; Roberts, J. M.; Scheidt, K. A. *Org. Lett.* **2010**, *12*, 2830.

(13) For selected examples of nucleophilic catalysis exploiting defluoronation/desilylation, see: (a) Bappert, E.; Müller, P.; Fu, G. C. *Chem. Commun.* **2006**, 2604. (b) Poisson, T.; Dalla, V.; Papamicael, C.; Dupas, G.; Marsais, F; Levacher, V. *Synlett* **2007**, 381. (c) Birrell, J. A.; Desrosier, J.-N.; Jacobsen, E. N. *J. Am. Chem. Soc.* **2011**, *133*, 13875. (d) Kalow, J. W.; Doyle, A. G. *J. Am. Chem. Soc.* **2011**, *133*, 16001.

(14) For computational studies on the stability of *β*-lactones and their highly asynchronous decarboxylation, see: (a) Morao, I.; Lecea, B.; Arrieta, A.; Cossío, F. P. *J. Am. Chem. Soc.* **1997**, *119*, 816. (b) Minato, T.; Yamabe, S. *J. Org. Chem.* **1983**, *48*, 1479. (c) Moyano, A.; Pericàs, M. A.; Valentí, E. *J. Org. Chem.* **1989**, *54*, 573.

(15) Frisch, M. J. et al. *Gaussian 09*, Revision A.1; Gaussian, Inc.: Wallingford, CT, 2009.

(16) (a) Lee, C.; Yang, W.; Parr, R. G. *Phys. Rev. B* **1988**, *37*, 785. (b) Becke, A. D. *J. Chem. Phys.* **1993**, *98*, 5648. For reviews of density-functional methods, see: (c) Ziegler, T. *Chem. Rev.* **1991**, *91*, 651. (d) *Density Functional Methods in Chemistry*; Labanowski, J. K., Andzelm, J. W., Eds.; Springer-Verlag: New York, 1991. (e) Parr, R. G.; Yang, W. *Density-Functional Theory of Atoms and Molecules*; Oxford University Press: New York, 1989. (f) Koch, W.; Holthausen, M. C. *A Chemist's Guide to Density Functional Theory*; Wiley−VCH: Weinheim, 2000.

(17) The B3LYP functional gives optimized molecular geometries of quantitative accuracy; for representative examples, see: (a) Wiest, O.; Montiel, D. C.; Houk, K. N. *J. Phys. Chem. A* **1997**, *101*, 8378. (b) Lilly, M. J.; Paddon-Row, M. N.; Sherburn, M. S.; Turner, C. I. *Chem. Commun.* **2000**, 2213. (c) Paddon-Row, M. N.; Sherburn, M. S. *Chem. Commun.* **2000**, 2215. (d) Kong, S.; Evanseck, J. D. *J. Am. Chem. Soc.* **2000**, *122*, 10418. (e) Tantillo, D. J.; Houk, K. N.; Jung, M. E. *J. Org. Chem.* **2001**, *66*, 1938. (f) Turner, C. I.; Williamson, R. M.; Paddon-Row, M. N.; Sherburn, M. S. *J. Org. Chem.* **2001**, *66*, 3963.

(18) (a) Miertuš, S.; Scrocco, E.; Tomasi, J. *Chem. Phys.* **1981**, *55*, 117−129. (b) Miertuš, S.; Tomasi, J. *Chem. Phys.* **1982**, *65*, 239−245. (c) Cossi, M.; Barone, V.; Cammi, R.; Tomasi, J. *Chem. Phys. Lett.* **1996**, *255*, 327−335. (d) Cammi, R.; Mennucci, B.; Tomasi, J. *J. Phys. Chem. A* **2000**, *104*, 5631−5637. (e) Cossi, M.; Scalmani, G.; Rega, N.; Barone, V. *J. Chem. Phys.* **2002**, *117*, 43.

(19) Zhao, Y.; Truhlar, D. G. *Theor. Chem. Acc.* **2008**, *120*, 215.

(20) Since the Michael reaction is accompanied by a transfer of −1*e*, from dienolate to acyl azolium cation, it is reasonable to expect a charge transfer of ca. −0.5*e* in the TS.

(21) For studies on the mechanism of thermal decarboxylation of *β*-lactones, see: (a) Mulzer, J.; Zippel, M. *Tetrahedron Lett.* **1980**, *21*, 751. (b) Mulzer, J.; Zippel, M. *J. Chem. Soc. Chem. Commun.* **1981**, 891.

(22) Curtiss, L. A.; Redfern, P. C.; Raghavachari, K. *J. Chem. Phys.* **2007**, *126*, 084108.

(23) Curtiss, L. A.; Redfern, P. C.; Raghavachari, K. *J. Chem. Phys.* **2007**, *127*, 124105.

(24) B3LYP calculated KIEs are known to correlate well to experimentally determined KIEs; for examples, see: (a) Beno, B. R.; Houk, K. N.; Singleton, D. A. *J. Am. Chem. Soc.* **1996**, *118*, 9984. (b) Acevedo, O.; Evanseck, J. D. *Org. Lett.* **2003**, *5*, 649.

(25) (a) Singleton, D. A.; Thomas, A. A. *J. Am. Chem. Soc.* **1995**, *117*, 9357. For studies using low conversion: (b) Frantz, D. E.; Singleton, D. A. *J. Am. Chem. Soc.* **2000**, *122*, 3288. (c) Denmark, S. E.; Pham, S. M.; Stavenger, R. A.; Su, X.; Wong, K.-T.; Nishigaichi, Y. *J. Org. Chem.* **2007**, *71*, 3904.

(26) For related approaches, see: (a) Gajewski, J. J.; Peterson, K. B.; Kagel, J. R. *J. Am. Chem. Soc.* **1987**, *109*, 5545. (b) Gajewski, J. J.; Peterson, K. B.; Kagel, J. R.; Huang, Y. C. J. *J. Am. Chem. Soc.* **1989**, *111*, 9078.

(27) Storer, J. W.; Raimondi, L.; Houk, K. N. *J. Am. Chem. Soc.* **1994**, *116*, 9675.

(28) Ryan, S. J.; Candish, L.; Martinez, I.; Lupton, D. W. *Aust. J. Chem.* **2011**, *64*, 1148.

(29) Chen, C.; Chien, C.-T.; Su, C.-H. *J. Fluor. Chem.* **2002**, *115*, 75.

(30) Kunetskiy, R. A.; Císarová, I.; Saman, D.; Lyapkalo, I. M. *Chem. Eur. J.* **2009**, *15*, 9477.

(31) Seguineau, P.; Villieras, J. *Tetrahedron Lett.* **1988**, *29*, 477.

(32) Kwart, H.; Gaffney, A. *J. Org. Chem.* **1983**, *48*, 4502.